Supporting Information

Potential Antimicrobial Isopropanol-Conjugated Carbazole Azoles as Dual Targeting Inhibitors of *Enterococcus faecalis*

Yuan Zhang,[†] Vijai Kumar Reddy Tangadanchu,[†] Yu Cheng,[†] Ren-Guo Yang,[‡] Jian-Mei Lin,[‡,*] and Cheng-He Zhou[†,*]

[†]Institute of Bioorganic & Medicinal Chemistry, Key Laboratory of Applied Chemistry of Chongqing Municipality, School of Chemistry and Chemical Engineering, Southwest University, Chongqing 400715, China

[‡]School of Medicine University of Electronic Science and Technology of China, Chengdu 610072, China

E-mail: zhouch@swu.edu.cn.

E-mail: linjianmei@med.uestc.edu.cn.

1. Experimental procedures

1.1. General methods

TLC (Thin-layer chromatography) analysis was performed through pre-coated silica gel plates. Melting points were recorded on X-6 melting point apparatus and uncorrected. FT-IR spectra were obtained from Bruker RFS100/S spectrophotometer (Bio-Rad, Cambridge, MA, USA) using KBr pellets in the 400−4000 cm^{-1} range. ^{1}H NMR and ^{13}C NMR were recorded on a Bruker AV 600 spectrometer with TMS as an internal standard. The chemical shifts were reported in parts per million (ppm), the coupling constants (*J*) are expressed in hertz (Hz) and signals were described as singlet (s), doublet (d), triplet (t), broad (br) as well as multiplet (m). The high-resolution mass spectra (HRMS) were recorded on IonSpec FT-ICR mass spectrometer with ESI resource.

Commercial carbazoles **1a**−**e** were deprotonated with potassium hydroxide, and the resulting anion reacted with epichlorohydrin to provide intermediates **2a**−**e** in 65.1−78.6% yields, which were further treated with various azoles in ethanol under reflux to afford carbazole derivatives **3a**−**e**, **4a**−**e**, and **5**−**6** with yields of 24.7−75.5%. It was noticed that under the same condition above methyl group containing imidazolyl carbazoles **4c** and **4d** were obtained in relatively low yields, which might be explained by the weak acidity of imidazole ring. Moreover, compounds **2f**−**g** were obtained from epoxide **2a** by using *N*-chlorosuccinimide (NCS) and *N*-bromosuccinimide (NBS) as chloration and bromination agents in *N*,*N*-dimetylformamide at room temperature. Subsequently, intermediates **2f**−**g** went through ring opening reaction using triazole and 2-methyl-5-nitro-1*H*-imidazole to afford final compounds **3f**−**g** and **4f**. Quantitative nuclear magnetic resonance (QNMR) method was employed to check the purity of the target compounds with 1,3,5-trioxane as internal standard and it was found that all the target compounds demonstrated a purity of more than 95%.

1.1.1. General procedure for the synthesis of compounds 2a–g

In a dry round bottom flask, various carbazoles **1a**–**e** (3 mmol, 1 equiv) was added to a solution of KOH (7.5 mmol, 2.5 equiv) in *N*,*N*-dimetylformamide (20 mL) at 4 ^{o}C. After stirring the mixture for 30 min at 4 ^{o}C, epichlorohydrin (3.6 mmol, 1.2 equiv) was added to the cooled flask drop-wise. The reaction was stirred at 4 ^{o}C overnight. The reaction heated to 25 ^{o}C, water (15 mL) was added to the mixture, and white solid precipitant formed. The mixture was filtered and washed with water (3 x 15 mL) to provide **2a–e**. Yields: 65.1–78.6%. To a solution of NCS or NBS (8.96 mmol, 2 equiv) in 10 mL *N*,*N*-dimetylformamide was added slowly to a suspension of 9-(oxiran-2-ylmethyl)-9*H*-carbazole **2a** (4.48 mmol, 1 equiv) in *N*,*N*-dimetylformamide (20 mL). The reaction mixture was stirred at room temperature and the progress of the reaction was monitored by TLC (petroleum ether/chloroform, 3/1, V/V). After the reaction was completed, the solution was washed with water (3 × 200 mL), the organic layer was dried under magnesium sulfate and filtered. The solvent was evaporated and the residue was dissolved in acetone (20 mL) and precipitated with hexane (60 mL). The crude products were filtered and dried under vacuum to afford desired

3,6-dichoro-9-(oxiran-2-ylmethyl)-9*H*-carbazole **2f** and 3,6-dibromo-9-(oxiran-2-ylmethyl)-9*H*-carbazole **2g** in yields of 45.3% and 50.7%, respectively.

1.1.2. Synthesis of 1-(9*H*-carbazol-9-yl)-3-(1*H*-1,2,4-triazol-1-yl)propan-2-ol (3a)

To a stirred solution of triazole (0.186 g, 2.7 mmol) and potassium carbonate (0.608 g, 4.4 mmol) in ethanol was added intermediate **2a** (0.5 g, 2.2 mmol). The mixture was stirred at 80 °C for 5 h. After the reaction was completed (monitored by TLC, chloroform/methanol, 10/1, V/V), the solvent was removed under reduced pressure, and the residue was dissolved in ethyl acetate (20 mL) and extracted with water (3 × 20 mL). After that, the combined organic phase was dried over anhydrous sodium sulfate and concentrated under reduced pressure. The resulting residue was purified by silica gel column chromatography eluting with chloroform/acetone (5/1–3/1, V/V) to give the pure compound **3a** (0.336 g) as white solid. Yield: 52.3%. mp: 154–155 °C. ^{1}H NMR (600 MHz, $CDCl_3$) δ 7.94 (d, *J* = 7.7 Hz, 2H, carbazole-4,5-*H*), 7.45 (d, *J* = 9.2 Hz, 2H, carbazole-1,8-*H*), 7.37 (t, *J* = 7.6 Hz, 2H, carbazole-2,7-*H*), 7.29 (d, *J* = 8.1 Hz, 2H, triaozle-3,5-*H*), 7.14 (t, *J* = 7.3 Hz, 2H, carbazole-3,6-*H*), 4.33 (d, *J* = 5.0 Hz, 1H, trizole-CH_2), 4.20 (d, *J* = 6.0 Hz, 2H, carbazole-CH_2), 4.02 (d, *J* = 11.5 Hz, 1H, trizole-CH_2), 3.89 (dd, *J* = 13.8, 8.1 Hz, 1H, chiral-*H*) ppm; ^{13}C NMR (151 MHz, $CDCl_3$) δ 151.47, 143.92, 140.57, 126.00, 123.04, 120.39, 119.53, 108.88, 68.77, 53.07, 46.67 ppm; HRMS (ESI): calcd for $C_{17}H_{16}N_4O$ $[M+H]^+$, 293.1402, found, 293.1404.

1.1.3. Synthesis of 1-(2-bromo-9*H*-carbazol-9-yl)-3-(1*H*-1,2,4-triazol-1-yl)propan-2-ol (3b)

Compound **3b** (0.245 g) was prepared as white solid according to the procedure described for compound **3a** starting from triazole (0.137 g, 1.99 mmol) and intermediate **2b** (0.5 g, 1.65 mmol). Yield: 67.4 %. mp: 174–175 °C. ^{1}H NMR (600 MHz, DMSO-d_6) δ 8.49 (s, 1H, triazole-5-*H*), 8.16 (d, *J* = 7.7 Hz, 1H, carbazole-4-*H*), 8.10 (d, *J* = 8.2 Hz, 1H, carbazole-5-*H*), 8.01 (s, 1H, triazole-3-*H*), 7.90 (s, 1H, carbazole-1-*H*), 7.63 (d, *J* = 8.2 Hz, 1H, carbazole-8-*H*), 7.48 (t, *J* = 7.7 Hz, 1H, carbazole-7-*H*), 7.34 (d, *J* = 8.2 Hz, 1H, carbazole-3-*H*), 7.23 (t, *J* = 7.4 Hz, 1H, carbazole-6-*H*), 5.45 (s, 1H, CHO*H*), 4.50 (d, *J* = 12.9 Hz, 1H, chiral-*H*), 4.46–4.36 (m, 2H, carbazole-CH_2), 4.31–4.29 (m, 2H, triazole-CH_2) ppm; ^{13}C NMR (151 MHz, DMSO-d_6) δ 156.54, 150.10, 146.82, 145.97, 131.36, 126.99, 126.91, 126.84, 126.82, 126.60, 125.54, 124.65, 123.74, 117.89, 115.18, 73.33, 57.94, 52.02 ppm; HRMS (ESI): calcd for $C_{17}H_{15}BrN_4O$ $[M+Na]^+$, 393.0327, found, 393.0328.

1.1.4. Synthesis of 1-(3-bromo-9*H*-carbazol-9-yl)-3-(1*H*-1,2,4-triazol-1-yl)propan-2-ol (3c)

Compound **3c** (0.315 g) was prepared as white solid according to the procedure described for compound **3a** starting from triazole (0.137 g, 1.99 mmol) and intermediate **2c** (0.5 g, 1.65 mmol). Yield: 60.9%. mp: 191–192 °C. ^{1}H NMR (600 MHz, DMSO-d_6) δ 8.46 (s, 1H, triazole-5-*H*), 8.39 (d, *J* = 1.8 Hz, 1H, carbazole-5-*H*), 8.20 (d, *J* = 7.8 Hz, 1H, carbazole-8-*H*), 7.99 (s, 1H, triazole-3-*H*), 7.63 (d, *J* = 8.3 Hz, 1H, carbazole-1-*H*), 7.61 (d, *J* = 8.7 Hz, 1H, carbazole-2-*H*), 7.57 (s, 1H, carbazole-4-*H*), 7.48 (t, *J* = 7.7 Hz, 1H, carbazole-7-*H*), 7.22 (t, *J* = 7.5 Hz, 1H, carbazole-6-*H*), 5.44 (d, *J* = 5.4 Hz, 1H, CHO*H*), 4.49 (dd, *J* = 14.9, 3.6 Hz, 1H, carbazole-CH_2), 4.42–4.36 (m, 2H, carbazole-CH_2, triazole-CH_2), 4.32–4.26 (m, 2H, triazole-CH_2, chiral-*H*) ppm; ^{13}C NMR (151 MHz, DMSO-d_6) δ 151.75, 145.33, 141.37, 139.86, 128.37, 126.89, 124.56, 123.13, 121.65, 121.15, 119.75, 112.30, 111.43, 110.44, 68.53, 53.25, 47.25 ppm; HRMS (ESI): calcd for $C_{17}H_{15}BrN_4O$ $[M+Na]^+$, 393.0327, found, 393.0326.

1.1.5. Synthesis of 1-(3-iodo-9*H*-carbazol-9-yl)-3-(1*H*-1,2,4-triazol-1-yl)propan-2-ol (3d)

Compound **3d** (0.384 g) was prepared as yellow solid according to the procedure described for compound **3a** starting from triazole (0.119 g, 1.72 mmol) and intermediate **2d** (0.5 g, 1.43 mmol). Yield: 73.6 %. mp: 185–186 °C. ^{1}H NMR (600 MHz, DMSO-d_6) δ 8.54 (s, 1H, triazole-5-*H*), 8.47 (s, 1H, triazole-3-*H*), 8.19 (d, *J* = 7.7 Hz, 1H, carbazole-5-*H*), 8.00 (s, 1H, carbazole-4-*H*), 7.71 (d, *J* = 8.6 Hz, 1H, carbazole-8-*H*), 7.62 (d, *J* = 8.3 Hz, 1H, carbazole-1-*H*), 7.52–7.45 (m, 2H, carbazole-2,7-*H*), 7.23 (t, *J* = 7.4 Hz, 1H, carbazole-6-*H*), 5.49 (d, *J* = 5.4 Hz, 1H, CHO*H*), 4.49–4.46 (m, 1H, carbazole-CH_2), 4.40–4.36 (m, 2H, carbazole-CH_2, triazole-CH_2), 4.29–4.23 (m, 1H, triazole-CH_2), 4.02–3.94 (m, 1H, chiral-*H*) ppm; ^{13}C NMR (151 MHz, DMSO-d_6) δ 151.77, 145.25, 141.01, 140.27, 133.91, 131.05, 129.00, 126.84, 125.38, 121.46, 121.02, 119.90, 112.80, 110.32, 68.51, 53.26, 47.24 ppm; HRMS (ESI): calcd for $C_{17}H_{15}IN_4O$ $[M+Na]^+$, 441.0188, found, 441.0189.

1.1.6. Synthesis of 1-(3,6-di-tert-butyl-9*H*-carbazol-9-yl)-3-(1*H*-1,2,4-triazol-1-yl)propan-2-ol (3e)

Compound **3e** (0.313 g) was prepared as yellow solid according to the procedure described for compound **3a** starting from triazole (0.123 g, 1.79 mmol) and intermediate **2e** (0.5 g, 1.49 mmol). Yield: 54.7%. mp: 234–235 ºC. ^{1}H NMR (600 MHz, DMSO-d_6) δ 8.46 (s, 1H, triazole-5-*H*), 8.17 (s, 2H, carbazole-4,5-*H*), 7.97 (s, 1H, triazole-3-*H*), 7.50–7.46 (m, 4H, carbazle-1,2,7,8-*H*), 5.44 (d, *J* = 4.6 Hz, 1H, CHO*H*), 4.33 (m, 5H, carbazole-CH_2, triazole-CH_2, chiral-*H*), 1.41 (s, 18H, CH(CH_3)$_3$) ppm; ^{13}C NMR (151 MHz, DMSO-d_6) δ 151.75, 145.29, 141.64, 139.51, 123.58, 122.66, 116.63, 109.43, 71.79, 68.66, 63.18, 34.86, 32.38 ppm; HRMS (ESI): calcd for $C_{25}H_{32}N_4O$ $[M+Na]^+$, 427.2474, found, 427.2475.

1.1.7. Synthesis of 1-(3,6-dichloro-9*H*-carbazol-9-yl)-3-(1*H*-1,2,4-triazol-1-yl)propan-2-ol (3f)

Compound **3f** (0.204 g) was prepared as white solid according to the procedure described for compound **3a** starting from triazole (0.142 g, 2.05 mmol) and 3,6-dichlorocarbazole intermediate **2f** (0.5 g, 1.17 mmol). Yield: 47.4 %. mp: 151–152 ºC. ^{1}H NMR (600 MHz, DMSO-d_6) δ 8.51 (s, 1H, triazole-5-*H*), 8.30 (s, 1H, triazole-3-*H*), 8.21 (d, *J* = 7.7 Hz, 1H, carbazole-5-*H*), 7.98 (d, *J* = 4.8 Hz, 1H, carbazole-4-*H*), 7.69 (d, *J* = 4.7 Hz, 1H, carbazole-8-*H*), 7.51 (d, *J* = 8.5 Hz, 1H, carbazole-1-*H*), 7.48 (d, *J* = 7.8 Hz, 1H, carbazole-2-*H*), 7.20 (d, *J* = 8.2 Hz, 1H, carbazole-6-*H*), 5.40 (s, 1H, CHO*H*), 4.89–4.85 (m, 1H, carbazole-CH_2), 4.71–4.59 (m, 1H, carbazole-CH_2), 4.42–4.30 (m, 3H, triazole-CH_2, chiral-*H*) ppm; ^{13}C NMR (151 MHz, DMSO-d_6) δ 151.79, 145.37, 128.68, 127.94, 126.68, 120.22, 112.93, 111.18, 69.96, 53.25, 48.45 ppm; HRMS (ESI): calcd for $C_{17}H_{14}Cl_2N_4O$ $[M+Na]^+$, 383.0442, found, 383.0443.

1.1.8. Synthesis of 1-(3,6-dibromo-9*H*-carbazol-9-yl)-3-(1*H*-1,2,4-triazol-1-yl)propan-2-ol (3g)

Compound **3g** (0.291 g) was prepared as white solid according to the procedure described for compound **3a** starting from triazole (0.109 g, 1.57 mmol) and 3,6-dibromocarbazole intermediate **2g** (0.5 g, 1.31 mmol). Yield: 49.3 %. mp: 134–135 ºC. ^{1}H NMR (600 MHz, DMSO-d_6) δ 8.50 (s, 2H, carbazole-4,5-*H*), 8.46 (s, 1H, triazole-3-*H*), 8.00 (d, 2H, *J* = 2.1 Hz, carbazole2,7-*H*), 7.79 (s, 1H, triazole-5-*H*), 7.64 (d, *J* = 1.5 Hz, 2H, carbazole-1,8-*H*), 5.42 (d, *J* = 5.6 Hz, 1H, CHO*H*), 4.91 (d, *J* = 14.5 Hz, 1H, carbazole-CH_2), 4.58 (d, *J* = 11.5 Hz, 1H, carbazole-CH_2), 4.39 (dd, *J* = 17.6, 11.2 Hz, 3H, triazole-CH_2, chiral-*H*) ppm; ^{13}C NMR (151 MHz, DMSO-d_6) δ 151.66, 145.38, 133.18, 130.06, 123.50, 123.24, 113.67, 112.77, 111.85, 69.77, 52.83, 47.87 ppm; HRMS (ESI): calcd for $C_{17}H_{14}Br_2N_4O$ $[M+Na+2]^+$, 472.9432, found, 472.9433.

1.1.9. Synthesis of 1-(9*H*-carbazol-9-yl)-3-(1*H*-imidazol-1-yl)propan-2-ol (4a)

Compound **4a** (0.225 g) was prepared as white solid according to the procedure described for compound **3a** starting from imidazole (0.184 g, 2.7 mmol) and compound **2a** (0.5 g, 2.2 mmol). Yield: 65.2%. mp: 162–163 ºC. ^{1}H NMR (600 MHz, $CDCl_3$) δ 8.04 (d, *J* = 7.7 Hz, 2H, carbazole-4,5-*H*), 7.43 (t, *J* = 7.5 Hz, 2H, carbazole-2,7-*H*), 7.37 (d, *J* = 8.1 Hz, 2H, carbazole-1,8-*H*), 7.21 (t, *J* = 7.3 Hz, 2H, carbazole-3,6-*H*), 7.11 (s, 1H, imidazole-2-*H*), 6.71 (d, *J* = 14.3 Hz, 2H, imidazole-4,5-*H*), 4.71 (s, 1H, CHO*H*), 4.40–4.25 (m, 3H, carbazole-CH_2, imidazole-CH_2), 3.93–3.80 (m, 2H, imidazole-CH_2 chiral-*H*) ppm; ^{13}C NMR (151 MHz, $CDCl_3$) δ 140.61, 137.29, 128.24, 125.98, 123.09, 120.39, 119.66, 119.47, 108.85, 69.54, 51.50, 47.08 ppm; HRMS (ESI): calcd for $C_{18}H_{17}N_3O$ $[M+H]^+$, 292.1450, found, 292.1449.

1.1.10. Synthesis of 1-(9*H*-carbazol-9-yl)-3-(4-nitro-1*H*-imidazol-1-yl)propan-2-ol (4b)

Compound **4b** (0.285 g) was prepared as yellow solid according to the procedure described for compound **3a** starting from 4-nitro-1*H*-imidazole (0.305 g, 2.7 mmol) and compound **2a** (0.5 g, 2.2 mmol). Yield: 48.9%. mp: 231–232 ºC. ^{1}H NMR (600 MHz, DMSO-d_6) δ: 8.39 (s, 1H, imidazole-5-*H*), 8.14 (d, *J* = 7.6 Hz, 2H, carbazole-4,5-*H*), 7.83 (s, 1H, imidazole-2-*H*), 7.65 (d, *J* = 8.1 Hz, 2H, carbazole-1,8-*H*), 7.45 (t, *J* = 7.6 Hz, 2H, carbazole-2,7-*H*), 7.21 (t, *J* = 7.4 Hz, 2H, carbazole-3,6-*H*), 5.50 (s, 1H, CHO*H*), 4.46 (dd, *J* = 14.8, 3.0 Hz, 1H, carbazole-CH_2), 4.42–4.32 (m, 2H, imidazole-CH_2), 4.30 (s, 1H, chiral-*H*), 4.15 (dd, *J* = 13.4, 9.0 Hz, 1H, carbazole-CH_2) ppm; ^{13}C NMR (151 MHz, DMSO-d_6) δ: 141.25, 138.36, 126.09, 122.74, 122.46, 120.54, 119.31, 68.97, 52.16, 47.11 ppm; HRMS (ESI): calcd for $C_{18}H_{16}N_4O_3$ $[M+Na]^+$, 359.1120, found, 359.1123.

1.1.11. Synthesis of 1-(9*H*-carbazol-9-yl)-3-(2-methyl-5-nitro-1*H*-imidazol-1-yl)propan-2-ol (4c)

Compound **4c** (0.285 g) was prepared as yellow solid according to the procedure described for compound **3a** starting from 2-methyl-5-nitro-1*H*-imidazole (0.343 g, 2.7 mmol) and compound **2a** (0.5 g, 2.2 mmol). Yield: 36.3%. mp: 161–162 ºC. ^{1}H NMR (600 MHz, DMSO-d_6) δ 8.31 (s, 1H, imidazole-4-*H*), 8.14 (d, *J* = 7.7 Hz, 2H, carbazole-4,5-*H*), 7.68 (d, *J* = 8.2 Hz, 2H, carbazole-1,8-*H*), 7.45 (t, *J* = 7.6 Hz, 2H, carbazole-2,7-*H*), 7.20 (t, *J* = 7.4 Hz, 2H, carbazole-3,6-*H*), 5.46 (d, *J* = 5.6 Hz, 1H,

CHO*H*), 4.49 (dd, *J* = 15.0, 3.4 Hz, 1H, carbazole-CH_2), 4.40 (dd, *J* = 14.9, 7.9 Hz, 1H, carbazole-CH_2), 4.27 (d, *J* = 12.3 Hz, 2H, imidazole-CH_2), 4.12–4.07 (m, 1H, chiral-*H*), 2.35 (s, 3H, imidazole-CH_3) ppm; ^{13}C NMR (151 MHz, DMSO-d_6) δ 146.08, 141.22, 126.03, 123.07, 122.71, 120.48, 119.35, 110.37, 69.92, 51.17, 47.12, 13.23 ppm; HRMS (ESI): calcd for $C_{19}H_{18}N_4O_3$ $[M+Na]^+$, 373.1277, found, 373.1278.

1.1.12. Synthesis of 1-(9*H*-carbazol-9-yl)-3-(2-methyl-1*H*-imidazol-1-yl)propan-2-ol (4d)

Compound **4d** (0.170 g) was prepared as white solid according to the procedure described for compound **3a** starting from 2-methyl-1*H*-imidazole (0.221 g, 2.7 mmol) and compound **2a** (0.5 g, 2.2 mmol). Yield: 24.7%. mp: 200–201 ºC. ^{1}H NMR (600 MHz, DMSO-d_6) δ 8.14 (d, *J* = 7.7 Hz, 2H, carbazole-4,5-*H*), 7.58 (d, *J* = 8.2 Hz, 2H, carbazole-1,8-*H*), 7.43 (t, *J* = 7.6 Hz, 2H, carbazole-2,7-*H*), 7.19 (t, *J* = 7.4 Hz, 2H, carbazole-3,6,-*H*), 7.10 (s, 1H, imidazole-4-*H*), 6.75 (s, 1H, imidazole-5-*H*), 5.40 (s, 1H, CHO*H*), 4.37 (m, 2H, carbazole-CH_2), 4.17 (s, 1H, chiral-*H*), 4.08 (d, *J* = 14.1 Hz, 1H, imidazole-CH_2), 3.99 (dd, *J* = 14.1, 8.2 Hz, 1H, imidazole-CH_2), 2.23 (s, 3H, imidazole-CH_3) ppm; ^{13}C NMR (151 MHz, DMSO-d_6) δ 144.84, 141.08, 126.39, 125.90, 122.55, 120.82, 120.44, 119.24, 110.14, 69.98, 50.03, 47.20, 13.49 ppm; HRMS (ESI): calcd for $C_{19}H_{19}N_3O$ $[M+H]^+$, 306.1606, found, 306.1608.

1.1.13. Synthesis of 1-(9*H*-carbazol-9-yl)-3-(2-phenyl-1*H*-imidazol-1-yl)propan-2-ol (4e)

Compound **4e** (0.360 g) was prepared as yellow solid according to the procedure described for compound **3a** starting from 2-phenyl-1*H*-imidazole (0.388 g, 2.7 mmol) and compound **2a** (0.5 g, 2.2 mmol). Yield: 43.5%. mp: 187–188 ºC. ^{1}H NMR (600 MHz, DMSO-d_6) δ 8.17 (d, *J* = 7.7 Hz, 2H, carbazole-4,5-*H*), 7.52 (d, *J* = 8.2 Hz, 2H, carbazole-1,8-*H*), 7.47 (d, *J* = 7.9 Hz, 2H, carbazole-2,7-*H*), 7.44 (d, *J* = 7.8 Hz, 2H, carbazole-3,6-*H*), 7.40 (s, 1H, imidazole-4-*H*), 7.31 (t, *J* = 7.3 Hz, 1H, Ph-4-*H*), 7.24–7.20 (m, 4H, Ph-2,3,5,6-*H*), 7.04 (s, 1H, imidazole-5-*H*), 5.70 (d, *J* = 4.8 Hz, 1H, CHO*H*), 4.36 (d, *J* = 4.0 Hz, 2H, carbazole-CH_2), 4.28 (s, 1H, chiral-*H*), 4.25–4.16 (m, 2H, imidazole-CH_2) ppm; ^{13}C NMR (151 MHz, DMSO-d_6) δ 147.28, 140.52, 131.06, 128.83, 128.69, 128.58, 128.15, 125.92, 123.19, 122.64, 120.44, 119.34, 109.95, 69.73, 50.87, 47.43 ppm; HRMS (ESI): calcd for $C_{24}H_{21}N_3O$ $[M+H]^+$, 368.1763, found, 368.1765.

1.1.14. Synthesis of 1-(3,6-dibromo-9*H*-carbazol-9-yl)-3-(2-methyl-5-nitro-1*H*-imidazol-1-yl)propan-2-ol (4f)

Compound **4f** (0.225 g) was prepared as yellow solid according to the procedure described for compound **3a** starting from 2-methyl-5-nitro-1*H*-imidazole (0.2 g, 1.57 mmol) and 3,6-dibromocarbazole intermediate **2g** (0.5 g, 1.31 mmol). Yield: 38.3%. mp: >250 ºC. ^{1}H NMR (600 MHz, DMSO-d_6) δ 8.48 (s, 2H, carbazole-4,5-*H*), 8.31 (s, 1H, imidazole-4-*H*), 7.71 (d, *J* = 8.7 Hz, 2H, carbazole-2,7-*H*), 7.63 (d, *J* = 10.1 Hz, 2H, carbazole-1,8-*H*), 5.45 (d, *J* = 5.7 Hz, 1H, CHO*H*), 4.51 (d, *J* = 14.8 Hz, 1H, carbazole-CH_2), 4.40 (dd, *J* = 14.9, 8.4 Hz, 1H, carbazole-CH_2), 4.28 (d, *J* = 13.8 Hz, 1H, imidazole-CH_2), 4.21 (s, 1H, chiral-*H*), 4.08 (dd, *J* = 13.9, 9.4 Hz, 1H, imidazole-CH_2), 2.51 (s, 3H, imidazole-CH_3) ppm; ^{13}C NMR (151 MHz, DMSO-d_6) δ 146.14, 145.79, 140.20, 129.16, 123.69, 123.58, 123.05, 112.77, 111.87, 69.33, 50.82, 47.39, 13.41 ppm; HRMS (ESI): calcd for $C_{19}H_{16}Br_2N_4O_3$ $[M+Na+2]^+$, 530.9487, found, 530.9463.

1.1.15. Synthesis of 1-(1*H*-benzo[d]imidazol-1-yl)-3-(9*H*-carbazol-9-yl)propan-2-ol (5)

Compound **5** (0.578 g) was prepared as white solid according to the procedure described for compound **3a** starting from benzimidazole (0.318 g, 2.7 mmol) and compound **2a** (0.5 g, 2.2 mmol). Yield: 75.5%. mp: 157–158 ºC. ^{1}H NMR (600 MHz, DMSO-d_6) δ 8.20 (s, 1H, benzimidazole-2-*H*), 8.15 (d, *J* = 7.7 Hz, 2H, carbazole-4,5-*H*), 7.65 (d, *J* = 8.1 Hz, 3H, carbazole-1,8-*H*, benzimidazole-7-*H*), 7.60 (d, *J* = 7.8 Hz, 1H, benzimidazole-4-*H*), 7.45 (t, *J* = 7.6 Hz, 2H, carbazole-2,7-*H*), 7.24 (t, *J* = 7.4 Hz, 1H, carbazole-3-*H*), 7.21 (t, *J* = 6.8 Hz, 3H, carbazole-6-*H*, benzimidazole-5,6-*H*), 5.41 (d, *J* = 4.8 Hz, 1H, CHO*H*), 4.57–4.51 (m, 2H, carbazole-CH_2), 4.42 (m, 1H, chiral-*H*), 4.33 (t, *J* = 8.8 Hz, 2H, benzimidazole-CH_2) ppm; ^{13}C NMR (151 MHz, DMSO-d_6) δ 144.95, 141.26, 134.81, 125.88, 122.68, 122.64, 121.82, 120.56, 119.83, 119.25, 110.91, 110.28, 69.25, 48.97, 47.46 ppm; HRMS (ESI): calcd for $C_{22}H_{19}N_3O$ $[M+H]^+$, 342.1606, found, 342.1605.

1.1.16. Synthesis of 1-(9*H*-carbazol-9-yl)-3-(5-methyl-1*H*-tetrazol-1-yl)propan-2-ol (6)

Compound **6** (0.201 g) was prepared as pink solid according to the procedure described for compound **3a** starting from 5-methyl-1*H*-tetrazole (0.227 g, 2.7 mmol) and compound **2a** (0.5 g, 2.2 mmol). Yield: 28.8%. mp: 160–161 ºC. ^{1}H NMR (600

MHz, DMSO-d_6) δ 8.15 (d, *J* = 7.7 Hz, 2H, carbazole-4,5-*H*), 7.66 (d, *J* = 8.2 Hz, 2H, carbazole-1,8-*H*), 7.46 (t, *J* = 7.6 Hz, 2H, carbazole-2,7-*H*), 7.21 (t, *J* = 7.4 Hz, 2H, carbazole-3,6-*H*), 5.50 (d, *J* = 5.4 Hz, 1H, CHO*H*), 4.76 (m, 2H, carbazole-CH_2), 4.57 (t, *J* = 9.1 Hz, 1H, chiral-*H*), 4.49 (dd, *J* = 13.0, 6.7 Hz, 2H, imidazole-CH_2), 2.44 (s, 3H, imidazole-CH_3) ppm; ^{13}C NMR (151 MHz, DMSO-d_6) δ 162.46, 140.97, 126.11, 122.70, 120.60, 119.36, 110.15, 68.64, 56.80, 47.04, 10.80 ppm; HRMS (ESI): calcd for $C_{17}H_{17}N_5O$ $[M+Na]^+$, 330.1331, found, 330.1334.

2. Biological assay procedures

Minimal inhibitory concentration (MIC, μg/mL) is defined as the lowest concentration of target compounds that completely inhibited the growth of bacteria and fungi, by means of standard two-fold serial dilution method in 96-well microtest plates according to the Clinical & Laboratory Standards Institute (CLSI). The tested microorganism strains were provided by the Clinical Laboratory Department, Sichuan Academy of Medical Sciences, Sichuan Provincial People's Hospital. Norfloxacin and fluconazole were used as control drugs. DMSO with inoculation bacterial not medicine was used as positive control to ensure that the solvent had no effect on bacteria growth. All the microbe growth was monitored visually and spectrophotometrically, and the experiments were performed in triplicate.

2.1. Antibacterial assay

The prepared compounds were evaluated for their antibacterial activities against Gram-positive bacteria (*Staphylococcus aureus*, Methicillin-Resistant *Staphylococcus aureus*, *Enterococcus faecalis*, *Staphylococcus aureus* ATCC 25923, *Staphylococcus aureus* ATCC 29213) and Gram-negative bacteria (*Klebsiella pneumonia*, *Escherichia coli*, *Acinetobacter baumanii*, *Pseudomonas aeruginosa*, *Pseudomonas aeruginosa* ATCC 27853, *Escherichia coli* ATCC 25922). The bacterial suspension was adjusted with sterile saline to a concentration of 1×10^5 CFU. Initially the compounds were dissolved in DMSO to prepare the stock solutions, then the tested compounds and reference drugs were prepared in Mueller-Hinton broth (Guangdong huaikai microbial sci. & tech co., Ltd, Guangzhou, Guangdong, China) to obtain the required concentrations of 512, 256, 128, 64, 32, 16, 8, 4, 2, 1, 0.5 μg/mL. These dilutions were inoculated and incubated at 37 ºC for 24 h. Antibacterial screening demonstrated that some of the target compounds could effectively inhibit the growth of the tested bacteria and exhibit broad antimicrobial spectrum. In general, intermediates **2a**–**g** exhibited weak to moderate activities against the tested bacteria in comparison with clinical drug, while the final compounds incorporated with azole ring displayed enhanced antibacterial effects on the whole.

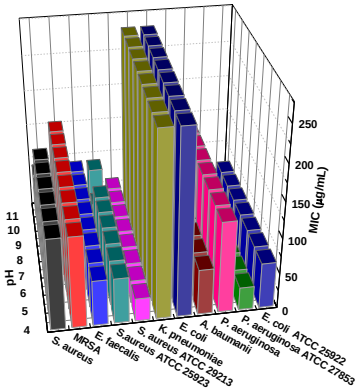

Figure S1. Antibacterial activities of compound 4c under different pH conditions.

Table S1. Antibacterial data as MIC (μg/mL) for intermediates 2a–g[a-c]

Compds	Gram-positive bacteria					Gram-negative bacteria					
	S. aureus	MRSA	*E. faecalis*	*S. aureus* 25923	*S. aureus* 29213	*K. pneumoniae*	*E. coli*	*A. baumanii*	*P. aeruginosa*	*P. aeruginosa* 27853	*E. coli* 25922
2a	256	>256	>256	128	128	128	>256	128	256	256	256
2b	128	256	256	64	64	64	256	256	128	256	128
2c	128	128	128	64	64	64	128	128	64	128	64
2d	256	128	256	128	128	128	256	128	256	128	64
2e	256	>256	>256	256	256	256	>256	256	256	256	256
2f	64	256	128	64	64	64	128	256	128	64	64

2g	128	256	256	128	128	128	256	256	128	128	128
A	2	8	4	1	8	4	16	8	2	0.5	8

[a] Minimal inhibitory concentrations were determined by micro broth dilution method for microdilution plates.

[b] *S. aureus*, *Staphylococcus aureus*; MRSA, Methicillin-Resistant *Staphylococcus aureus*; *E. faecalis*, *Enterococcus faecalis*; *S. aureus* 25923, *Staphylococcus aureus* ATCC 25923; *S. aureus* 29213, *Staphylococcus aureus* ATCC 29213; *K. pneumonia*, *Klebsiella pneumonia*; *E. coli*, *Escherichia coli*; *A. baumanii*, *Acinetobacter baumanii*; *P. aeruginosa*, *Pseudomonas aeruginosa*; *P. aeruginosa* 27853, *Pseudomonas aeruginosa* ATCC 27853; *E. coli* 25922, *Escherichia coli* ATCC 25922.

[c] A = Norfloxacin.

Table S2. Antibacterial data as MIC (μg/mL) for compounds 3–6

Compds	Gram-positive bacteria					Gram-negative bacteria					
	S. aureus	MRSA	*E. faecalis*	*S. areus* 25923	*S. aureus* 29213	*K. pneumoniae*	*E. coli*	*A. baumanii*	*P. aeruginosa*	*P. aeruginosa* 27853	*E. coli* 25922
3a	256	256	64	64	64	256	256	128	256	128	256
3b	128	128	32	32	32	128	128	64	128	64	128
3c	64	128	32	32	16	128	128	64	128	32	64
3d	128	256	32	64	64	256	256	128	256	64	128
3e	256	256	128	128	128	256	256	256	256	128	256
3f	64	32	2	16	4	64	64	128	64	16	8
3g	64	64	8	32	8	128	64	64	64	16	8
4a	128	256	256	128	128	256	256	64	128	32	128
4b	128	128	32	32	64	128	128	32	64	64	8
4c	128	256	64	64	32	128	128	64	128	32	32
4d	256	256	64	64	8	256	64	128	256	64	128
4e	256	256	128	256	256	256	128	256	256	256	256
4f	64	128	32	64	32	128	64	64	128	4	16
5	256	256	128	128	128	256	128	256	256	256	128
6	256	256	256	64	64	256	256	128	256	256	256
A	2	8	4	1	8	4	16	8	2	0.5	8

2.2. Antifungal assay

The newly synthesized compounds were evaluated for their antifungal activities against *Candida albicans*, *Candida tropicals*, *Aspergillus fumigatus*, *Candida albicans* ATCC 90023, *Candida parapsilosis* ATCC 22019. A spore suspension in sterile distilled water was prepared from one day old culture of the fungi growing on Sabouraud agar (SA) media. The final spore concentration was 1–5 × 10^3 spore mL^{-1}. From the stock solutions of the tested compounds and reference antifungal drug fluconazole, dilutions in sterile RPMI 1640 medium (Neuronbc Laboraton Technology CO, Ltd, Beijing, China) were made resulting in eleven wanted concentrations (0.5 to 512 μg/mL) of each tested compound. These dilutions were inoculated and incubated at 37 ºC for 24 hours.

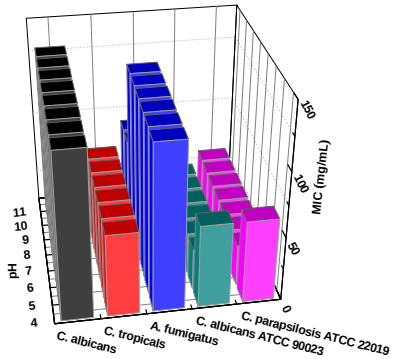

Figure S2. Antifugal activities of compound **4c** under different pH conditions.

Table S3. Antifungal data as MIC (μg/mL) for intermediates 2a–g[d]

Compds	Fungi				
	C. albicans	*C. tropicals*	*A. fumigatus*	*C. albicans ATCC 90023*	*C. parapsilosis ATCC 22019*
2a	>256	>256	256	256	256
2b	256	256	256	128	128
2c	128	128	128	64	64
2d	>256	>256	256	128	128
2e	>256	256	256	256	256
2f	128	64	128	64	64
2g	256	128	128	128	64
Fluconazole	4	8	256	2	4

[d] *C. albican*s, *Candida albicans*; *C. tropical*, *Candida tropical*; *A. fumigatus*, *Aspergillus fumigatus*; *C. albicans* ATCC 90023, *Candida albicans* ATCC 90023; *C. parapsilosis* ATCC 22019, *Candida parapsilosis* ATCC 22019.

The antifungal data in Table S3 displayed that most of the target isopropanol-conjugated carbazole azoles revealed a similar tendency to their antibacterial activities. Triazolyl ethanols **3a–g** also behaved more active than imidazolyl ethanols **4a–f** in inhibiting the growth of tested fungi, revealing that triazole was positive to antifungal activities. It was noticeable that compound **3f** had comparable anti-*C. parapsilosis* ATCC 22019 (MIC = 4 μg/ 185 mL) and superior anti-*A. fumigatus* (MIC = 32 μg/mL) abilities to clinical fluconazole. It was surprising that nitroimidazole derivative **4f** could inhibit the growth of *A. fumigatus* at a low concentration of 16 μg/mL, and was 16 times superior to fluconazole, which suggested that compound **4f** might be further investigated as a promising candidate for the administration of *A. flavus* infection.

Table S4. Antifungal data as MIC (μg/mL) for compounds 3–6

Compds	Fungi				
	C. albicans	*C. tropicals*	*A. fumigatus*	*C. albicans ATCC 90023*	*C. parapsilosis ATCC 22019*
3a	256	128	256	128	128
3b	128	64	128	64	32
3c	64	64	128	32	8
3d	128	128	256	64	64
3e	256	256	>256	256	256
3f	64	32	32	16	4
3g	64	64	64	32	8
4a	256	128	>256	256	128
4b	128	64	128	32	16
4c	128	64	128	64	64
4d	256	256	256	128	128
4e	>256	>256	>256	256	256
4f	64	128	16	64	16
5	>256	>256	>256	>256	256
6	128	256	128	128	128
Fluconazole	4	8	256	2	4

4. Resistance study

E. faecalis was employed to develop antimicrobial resistance with compound **3f**. The *E. faecalis* strain was exposed to the increasing concentrations of compound **3f** from MIC for the sustained passages, and the new MIC values were determined every 24h after the propagation of *E. faecalis*. The initial MIC values of compound **3f** and antibiotic norfloxacin against *E. faecalis* were obtained as described above. Serial passage and MICs determination were performed in 96 well microtiter plate containing compounds, each over a range of doubling dilution concentrations. After the incubation period 18 h, the entire content of the triplicate wells with a concentration of compounds permitting visible growth was then used to prepare the bacterial dilution (approximately 2×10^5 CFU/mL) for the successive exposure. The experiment was repeated for 16 days. As a positive control, parallel cultures were exposed to two fold dilutions of the standard antibiotic norfloxacin.

5. Time kill kinetics

The rate of bactericidal activity was evaluated by performing time-kill kinetics. Briefly, *E. faecalis* bacterium was grown in suitable growth medium at 37 °C for 6 h and diluted in respective media. Compound **3f** was added to the bacterial solution (*E. faecalis* of approximately 1.8×10^5 CFU/mL) at concentrations of 4 × MIC in a 96-well plate. The plate was then incubated at 37 °C. At different time intervals (0, 1, 2, 3, 4, 5, 6 and 7 h), 20 mL of aliquots from the solution were taken out and serially diluted (10-fold serial dilution) in 0.9% saline. Then 20 mL of the dilutions was plated on respective agar plates and incubated at 37 °C for 24 h. The bacterial colonies were counted, and results are represented in logarithmic scale: $\log_{10}$ (CFU/mL) vs time (h).

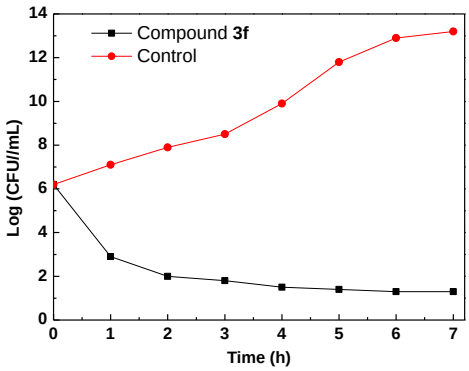

Figure S3. Time–kill kinetic of compound **3f** (4 × MIC) against *E. faecalis*.

6. Bacterial membrane disruption

The culture (mid log phase) of *E. faecalis* and *E. coli* ATCC 25922 was harvested (3500 rpm, 5 min), washed, and resuspended in 5 mM glucose and 5 mM HEPES buffer (pH 7.2) in 1:1 ratio after growth for 6 h. Then an amount of 10 mL of test compound **3f** (12 × MIC) was added to a cuvette containing 2 mL of bacterial suspension and 10 mM propidium iodide (PI). Fluorescence was monitored at excitation wavelength of 535 nm (slit width of 10 nm) and emission wavelength of 617 nm (slit width of 5 nm). As a measure of inner membrane permeabilization, the uptake of PI was monitored by the increase in fluorescence for 10 min. A control experiment was performed by treating the preincubated bacterial and dye solution only with water (10 mL).

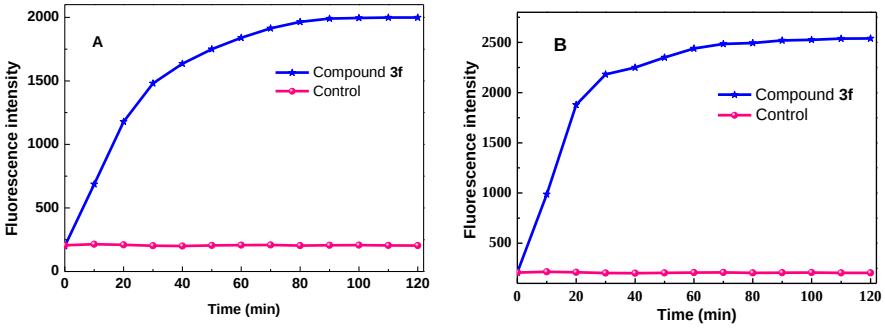

Figure S4. Membrane dysfunction ability of compound **3f** at concentration of 12 × MIC against: (A) *E. faecalis*; (B) *E. coli* ATCC 25922.

7. Cytotoxicity evaluation

RAW264.7 cells (Kunming wildlife cell bank of the Chinese academy of sciences, Kunming, China) were grown in H-DMEM medium supplemented with 10% (v/v) fetal bovine serum, 1% (v/v) penicillin/streptomycin solution and incubated at 37 °C in a humidified atmosphere containing 5% CO_2. The medium was changed every 2 days. For the cell viability assay, cells were seeded in fresh culture medium at a density of 3.5 × 104 cells/mL. Cell viability was measured using MTT assay. RAW264.7 cells (3.5 × 104 cells/mL) were seeded into 96-well flat bottom plates and incubated overnight prior to the experiment. By use of a Falcon 96-well, flat-bottom plate, 100 μL of the cell suspension was added to each of the wells and the cells were incubated for 24 h. Cells were cultured for 24 h in these solutions. The cell viability was examined by a microplate reader. Compound **3f** was dissolved in DMSO to prepare the stock solutions, and then the tested compound was prepared in medium to obtain the required concentrations of 8, 16, 32, 64, 128, 256 and 512 μg/mL, one containing no compound (non-treated cells) was applied as the

control. After incubation with compound 3f for 24 h, 10 μL of a 5 mg/mL solution of MTT in PBS was added to each well and further incubated for an additional 4 h. The supernatant was removed, and 150 μL DMSO was added to each well. Following oscillation for 10 min, absorbance values were measured at 490 nm by microplate reader (Tecan, Salzburg, Switzerland).

8. Interactions with DNA

8.1 DNA isolation and general procedures

The isolation of DNA from *E. faecalis* bacterium needs a four-step process:

(1) An overnight culture (1 mL) was added to a microcentrifuge tube (1.5 mL), and then centrifuged at 13,000–16,000 × *g* for 2 min to pellet the cells. The supernatant was removed and the cells were resuspended thoroughly in EDTA (480 μL, 50 mM). The lytic enzyme (120 μL) was added appropriately to the resuspended cell pellet, and mixed gently. Nuclei Lysis solution (600 μL) was added to the sample and it was gently pipeted until the cells are resuspended. RNase solution (3 μL) was added to the cell lysate, the tube was inverted to mix for 2–5 times. After the sample was incubated at 37 ^{o}C for 15–60 min, then it was cooled to room temperature. (2) Protein precipitation solution (200 μL) was added to the RNase-treated cell lysate, and vortex vigorously at high speed for 20 s to mix the protein precipitation solution with the cell lysate. (3) The supernatant containing the DNA was transfered to a clean microcentrifuge tube (1.5 mL) containing room temperature isopropanol (600 μL). The supernatant was carefully poured off and the tube was drained on a clean absorbent paper. The room temperature ethanol (70%, 600 μL) was added to the tube and it was gently inverted several times to wash the DNA pellet. (4) DNA rehydration solution (100 μL) was added to the tube and the DNA was rehydrated by incubating at 65 ^{o}C for 1 h. The solution was mixed periodically by gently tapping the tube. Alternatively, the DNA was rehydrated by incubating the solution overnight at room temperature or at 4 ^{o}C. The obtained DNA was stored at 2–8 ^{o}C.

UV spectra were recorded at room temperature on a TU-2450 spectrophotometer (Puxi Analytic Instrument Ltd. of Beijing, China) equipped with 1.0 cm quartz cells. NR was obtained from Sigma-Aldrich (Sigma Chemical Co., St. Louis, MO). Tris, HCl were analytical purity. Fluorescence spectra were recorded on F-7000 Spectrofluorimeter (Hitachi, Tokyo, Japan) equipped with 1.0 cm quartz cells, the widths of both the excitation and emission slit were set as 5 nm, and the excitation wavelength was 288 nm. Fluorescence spectra were recorded at 290 K in the range of 200–800 nm. Sample masses were weighed on a microbalance with a resolution of 0.1 mg. All other chemicals and solvents were commercially available, and used without further purification. *E. faecalis* DNA was used without further purification, and its stock solution was prepared by dissolving an appropriate amount of DNA in doubly distilled water. The solution was allowed to stand overnight and store at 4 ^{o}C in the dark for about a week. The concentration of DNA in stock solution was determined by UV absorption at 260 nm using a molar absorption coefficient ξ_{260} = 6600 L mol^{-1} cm^{-1} (expressed as molarity of phosphate groups) by Bouguer-Lambert-Beer law. The purity of DNA was checked by monitoring the ratio of the absorbance at 260 nm to that at 280 nm. The solution gave a ratio of > 1.8 at A_{260}/A_{280}, which indicated that DNA was sufficiently free from protein. NR stock solution was prepared by dissolving its solid in doubly distilled water and was kept in a cool and dark place. All the solutions were adjusted with Tris-HCl buffer solution (pH = 7.4), which was prepared by mixing and diluting Tris solution with HCl solution.

8.2 Absorption spectra

Hypochromism and hyperchromism have been acknowledged to be important spectral characteristics to distinguish the change of DNA double-helical structure in absorption spectroscopy. With a fixed concentration of DNA, UV–vis absorption spectra were recorded with the increasing amount of compound **3f**. The maximum absorption peak of DNA at 260 nm in Figure S5 showed a proportional increase accompanied by slightly red shift with the increasing concentration of compound **3f**. Meanwhile, the measured value of **3f**–DNA complex was lower than the sum of free DNA and free compound **3f**, suggesting a hypochromic effect between **3f** and DNA and further demonstrating a close proximity of the aromatic chromophore to the DNA bases (inset of Figure S5), where the intercalation of the aromatic chromophore of compound **3f** into the helix and the strong overlap of π-π* states in the large π-conjugated system with the electronic states of DNA bases could be observed as a result of noncovalent interactions. The hypochromism and slightly red shift preliminarily confirmed an intercalative action mode between DNA and compound **3f**.

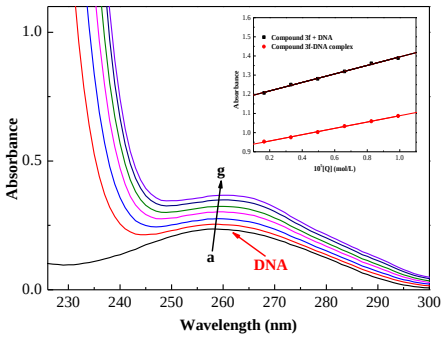

Figure S5. UV absorption spectra of various concentrations of compound **3f**. *c*(compound **3f**)/(10^{-5} mol·L^{-1}), *a*–*h*: from 0 to 0.99 at increment of 0.165.

On the basis of the variations in the absorption spectra of DNA upon binding to **3f**, equation 1 can be utilized to calculate the intrinsic binding constant (K)[1].

$$\frac{A^0}{A-A^0} = \frac{\xi_C}{\xi_{D-C}-\xi_C} + \frac{\xi_C}{\xi_{D-C}-\xi_C} \times \frac{1}{K[Q]} \quad (1)$$

A^0 and A represent the absorbance of DNA in the absence and presence of compound **3f** at 260 nm, ξ_C and $\xi_{D\text{-}C}$ are the absorption coefficients of compound **3f** and **3f**–DNA complex respectively. The plot of $A^0/(A–A^0)$ versus 1/[compound **3f**] is constructed by using the absorption titration data and linear fitting (Figure S6), yielding the binding constant, K = 3.17 × 10^4 L/mol, R = 0.9987, SD = 0.2152 (R is the correlation coefficient, and SD is standard deviation).

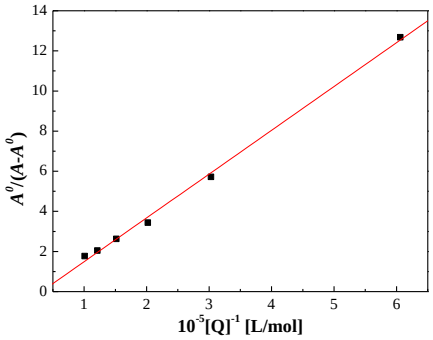

Figure S6. The plot of $A^0/(A–A^0)$ versus 1/[compound **3f**].

Further exploration of action mode between carbazole based triazolyl ethanol **3f** and DNA was carried out by employing low toxic, highly stable and convenient neutral red (NR) as a spectral probe, which has been evidenced to bind with DNA in an intercalative binding type[2]. The absorption spectra of the NR dye upon the addition of DNA (Figure S7) demonstrated that the absorption peak of the NR at around 460 nm presented gradual decrease along with the increasing concentration of DNA, and a new band appeared around 530 nm, which suggested the formation of the new DNA–NR complex. This was further evidenced by the isosbestic point at 504 nm. The absorption spectrum (Figure S8) showed a competitive binding between between NR and **3f** with DNA. With the increasing concentration of **3f**, the maximum absorption around 530 nm decreased presented a reverse process in comparison with the absorption of free NR in the presence of the increasing concentrations of DNA. This suggested that compound **3f** could intercalate into the double helix of DNA by emulatively substituting NR in NR–DNA complex, which further block DNA replication and thus exert the antimicrobial activities. Moreover, the increase of absorbance around 276 nm further proved the intercalation of compound **3f** into DNA.

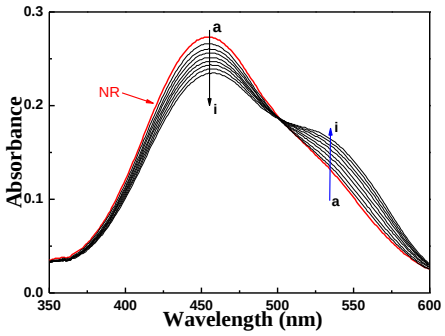

Figure S7. UV absorption spectra of NR in the presence of DNA at pH 7.4 and room temperature. c(NR) = 2 × 10^{-5} mol/L, and c(DNA) = 0–3.84 × 10^{-5} mol/L for curves a–i respectively at increment 0.48 × 10^{-5}.

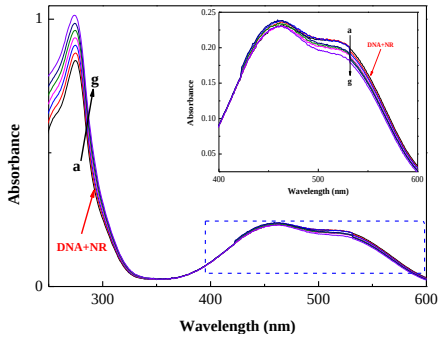

Figure S8. UV absorption spectra of the competitive reaction between **3f** and neutral red with DNA. c(DNA) = 4.0 × 10^{-5} mol/L, c(NR) = 2 × 10^{-5} mol/L, and c(compound **3f**) = 0–0.99 × 10^{-5} mol/L for curves a–g respectively at an increment of 0.165 × 10^{-5} mol/L. Inset: absorption spectra of the system with the increasing concentration of **3f** in the wavelength range of 400–600 nm absorption spectra of competitive reaction between compound **3f** and NR with DNA.

8.3 Iodide quenching experiments

Steady-state emission quenching experiments is thought to be capable of further confirming about the binding of compound **3f** with DNA. If a molecule is protected from being quenched by anionic quencher with the existence of anionic quencher, the binding of the small molecule with DNA belongs to an intercalative mode. Moreover, the Stern-Volmer plots get changed with the addition of DNA, which is attributed to the repulsions between the negative charged quencher and the DNA polyanion backbone. This hinders the access of the I^- ion to the DNA bound complexes. A larger slope for the Stern-Volmer curve means poorer protection and lower binding[3,4]. In this work, negatively charged I^- ion was selected as quencher to give fluorescence quenching curves Figure S9 & S10 of compound **3f** in the absence and presence of DNA. It can be indicated that the addition of KI led to extensive quenching of the fluorescence intensity.

The quenching constant can be deduced from Stern-Volmer equation (2)[5]:

$$\frac{F_0}{F} = 1 + K_{SV}[Q] \qquad (2)$$

Where F_0 and F represent the fluorescence intensity of compound **3f**/**3f**–DNA system in the absence and presence of the quencher KI, respectively. K_{SV} (L·mol^{-1}) is the Stern-Volmer quenching constant, and [Q] is the concentration of KI. The Stern-Volmer equation was applied to determine K_{SV} by linear regression of a plot of F_0/F versus [Q] (inset of Figures S9 & S10). The observed quenching constant K_{SV} of 9.3 L/mol in the presence of DNA was higher than that of 14.4 L/mol without DNA. The fluorescence quenching of compound **3f** was reduced when compound **3f** was bound to the DNA helix, which reconfirmed that compound **3f** could act as an intercalator of DNA to disturb its biological function.

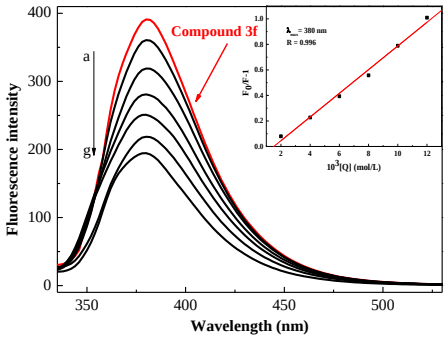

Figure S9. Fluorescence spectra of compound **3f** with increasing concentration of KI. *c*(compound **3f**) = 1.0 × 10^{-5} mol/L; *c*(KI) = 0–12 × 10^{-3} mol/L for curves a–g at an increment of 2 × 10^{-3} mol/L; T = 298 K, λex = 295 nm. Inset: Stern-Volmer plot of the fluorescence titration data of compound **3f**.

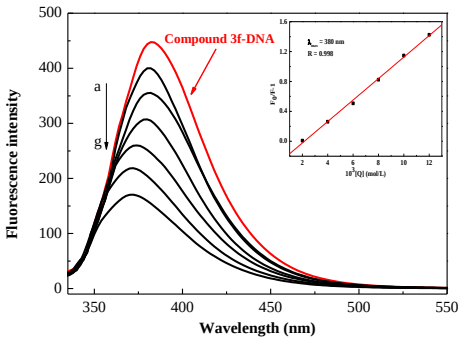

Figure S10. Fluorescence spectra of compound **3f** and DNA system with increasing concentration of KI. *c*(compound **3f**) = 1.0 × 10^{-5} mol/L; *c*(DNA) = 4 × 10^{-5} mol/L; *c*(KI) = 0–12 × 10^{-3} mol/L for curves a–g at an increment of 2 × 10^{-3} mol/L; T = 298 K, λex = 295 nm. Inset: Stern-Volmer plot of the fluorescence titration data of compound **3f** and DNA system.

9. Molecular docking

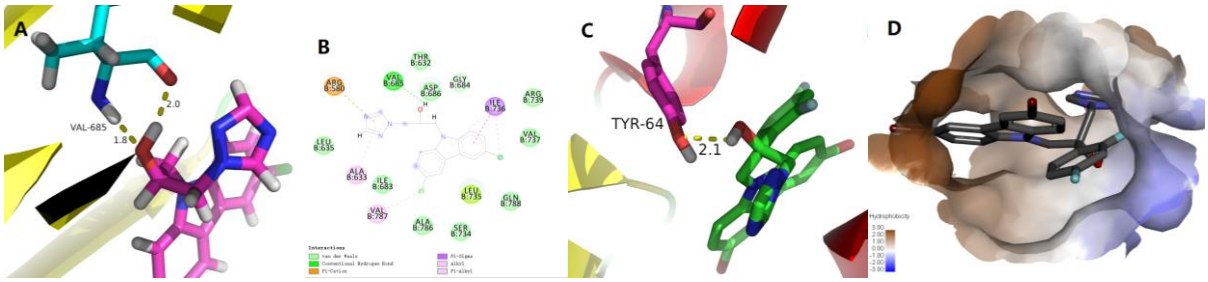

Figure S11. Molecular modeling of compound **3f** and DNA gyrase: (A) and (B) *S*-enantiomer; (C) and (D) *R*-enantiomer

10. Some spectra of target compounds

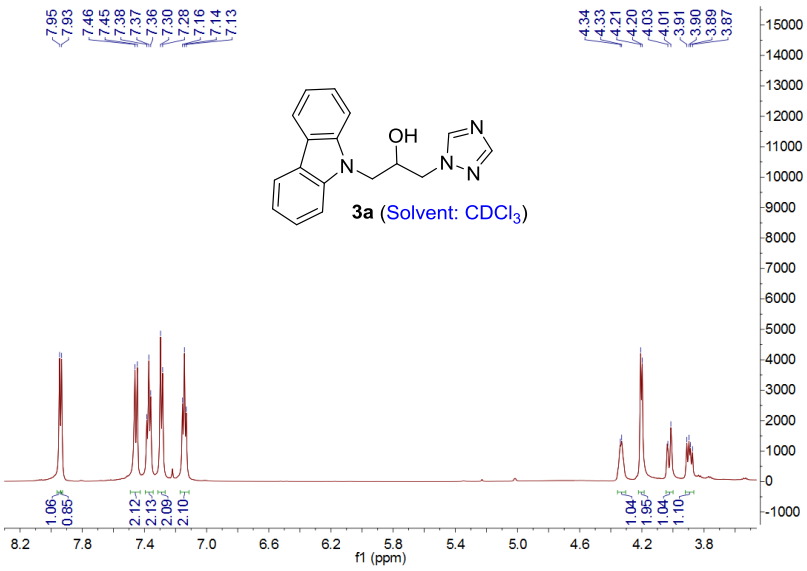

Figure S12. ^{1}H NMR spectrum of compound **3a**

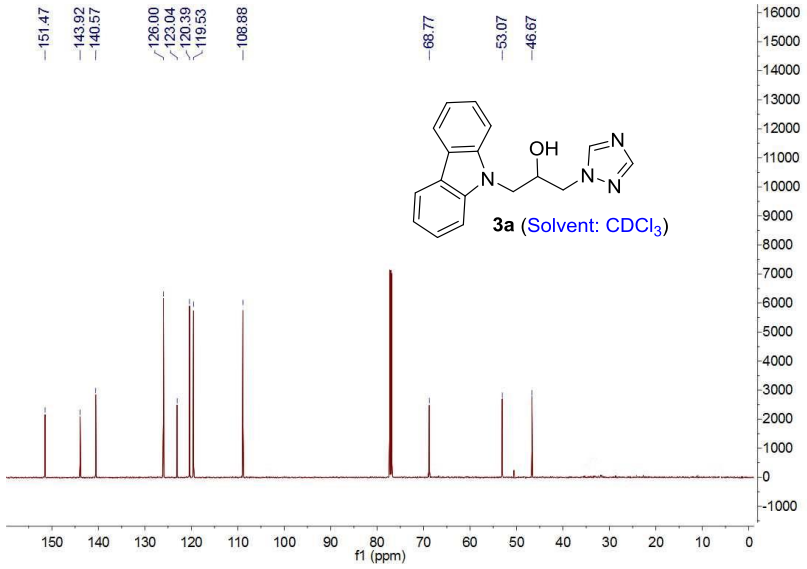

Figure S13. ^{13}C NMR spectrum of compound **3a**

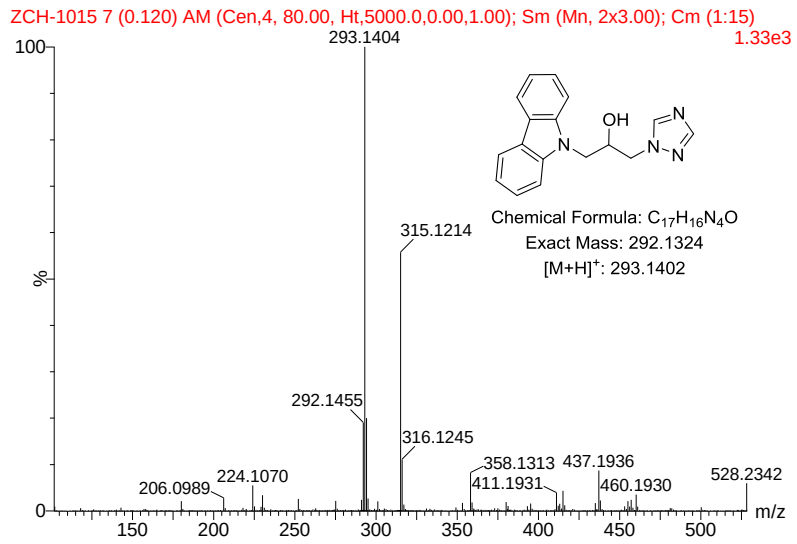

Figure S14. HRMS spectrum of compound **3a**

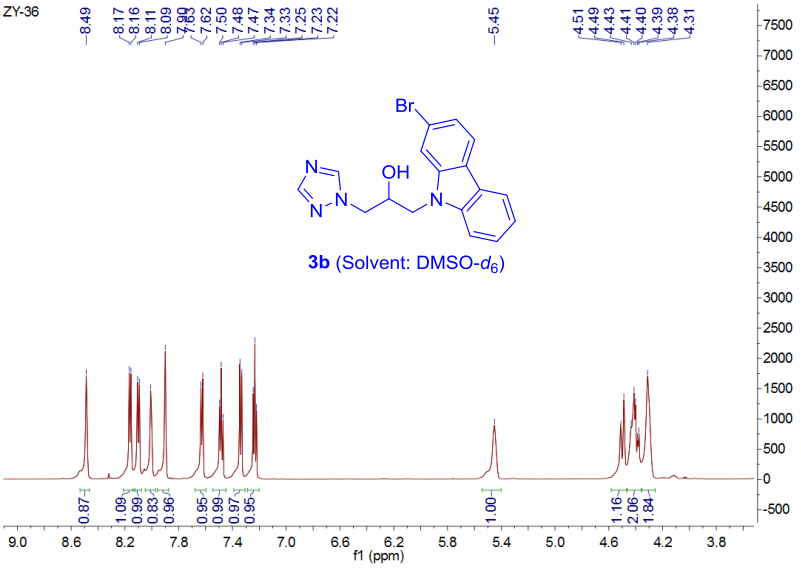

Figure S15. ^{1}H NMR spectrum of compound **3b**

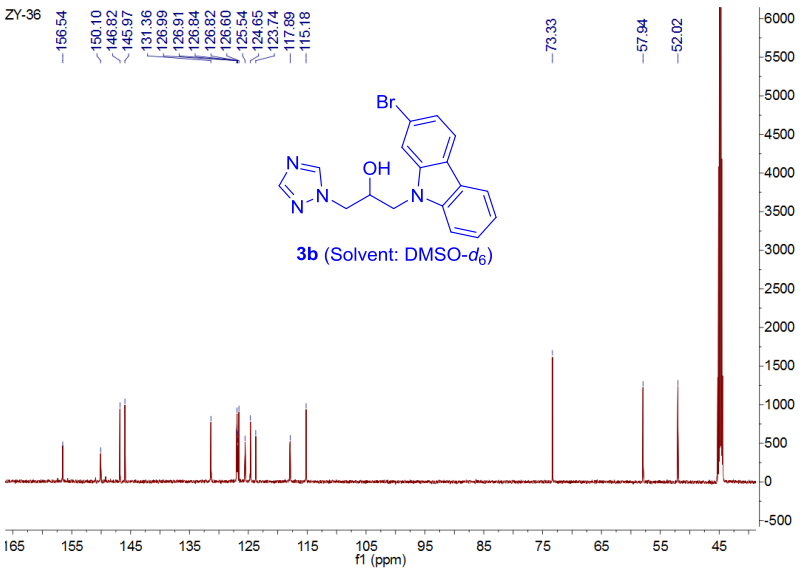

Figure S16. ^{13}C NMR spectrum of compound **3b**

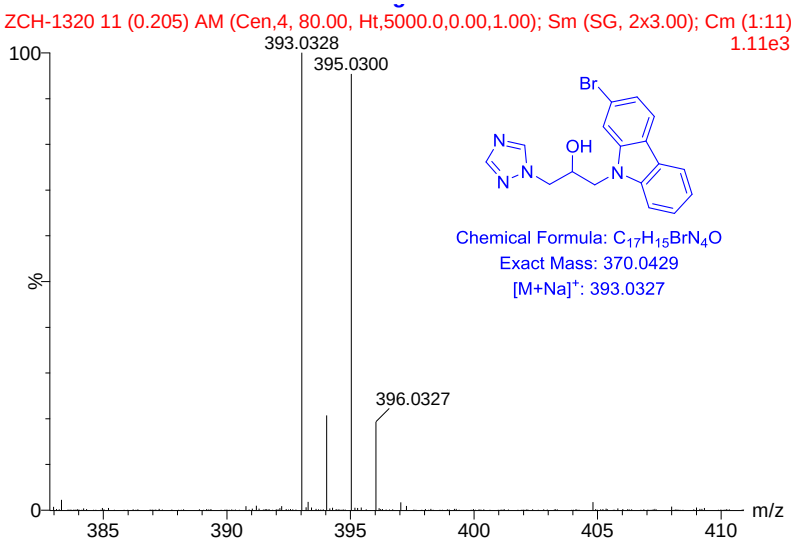

Figure S17. HRMS spectrum of compound **3b**

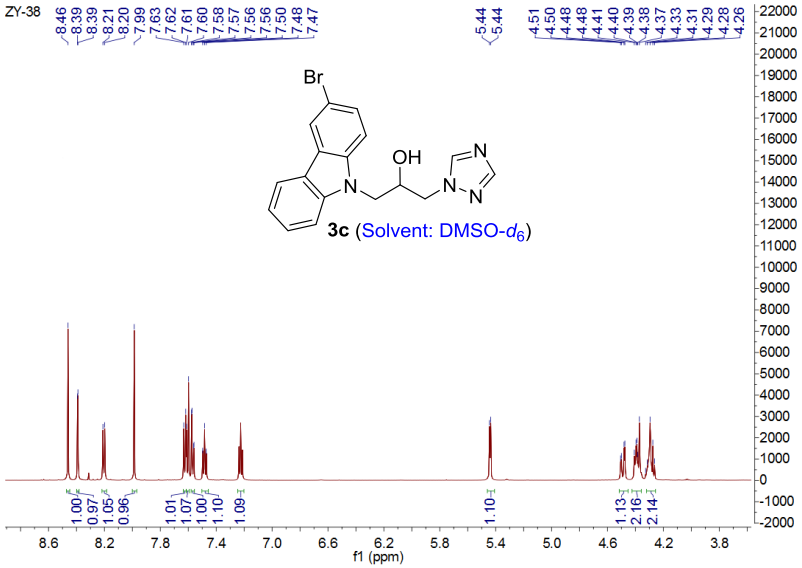

Figure S18. ^{1}H NMR spectrum of compound **3c**

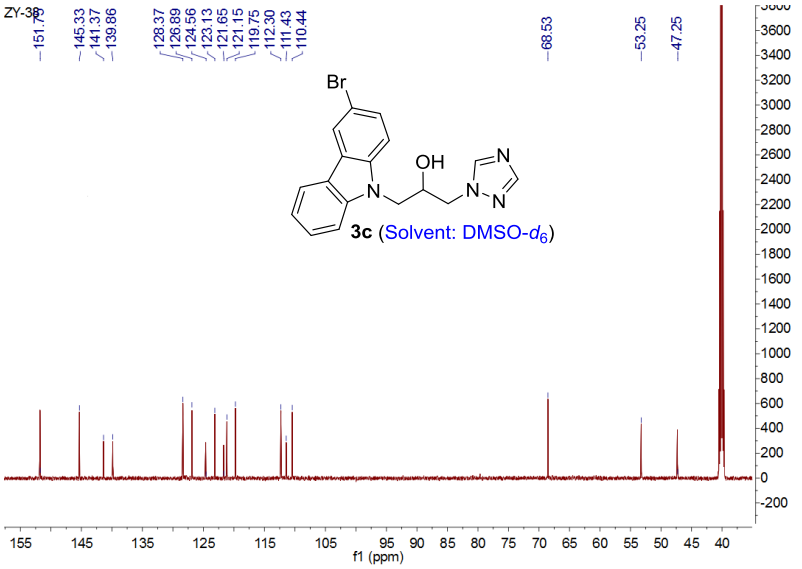

Figure S19. ^{13}C NMR spectrum of compound **3c**

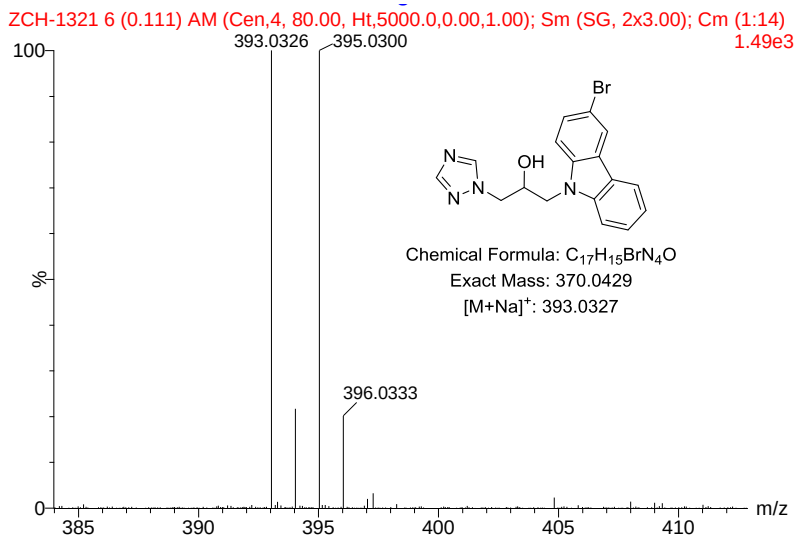

Figure S20. HRMS spectrum of compound **3c**

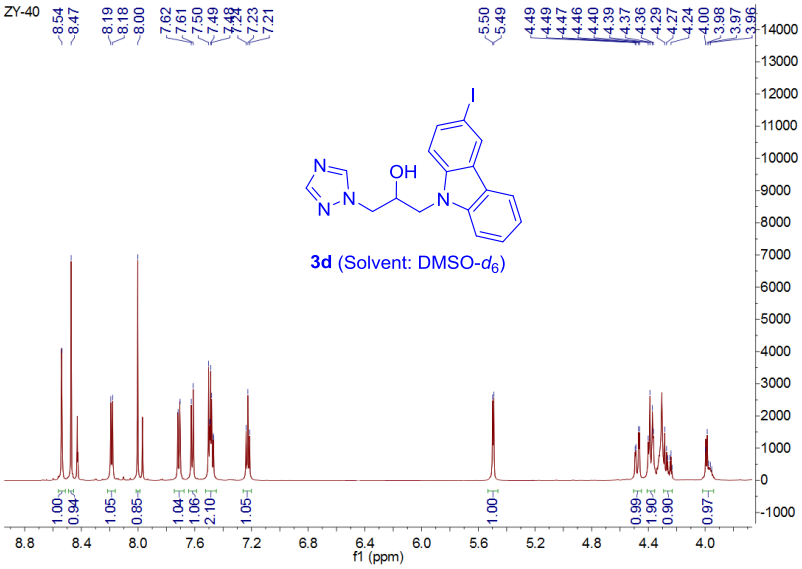

Figure S21. ^{1}H NMR spectrum of compound **3d**

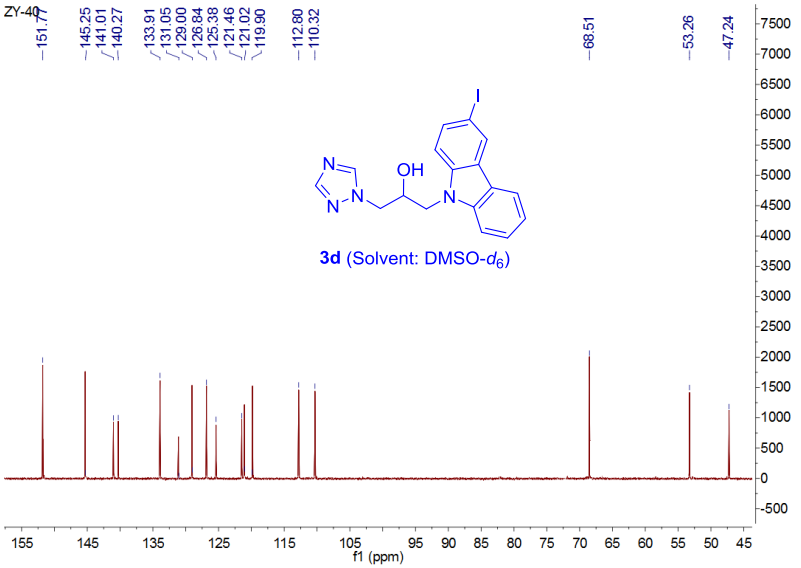

Figure S22. ^{13}C NMR spectrum of compound **3d**

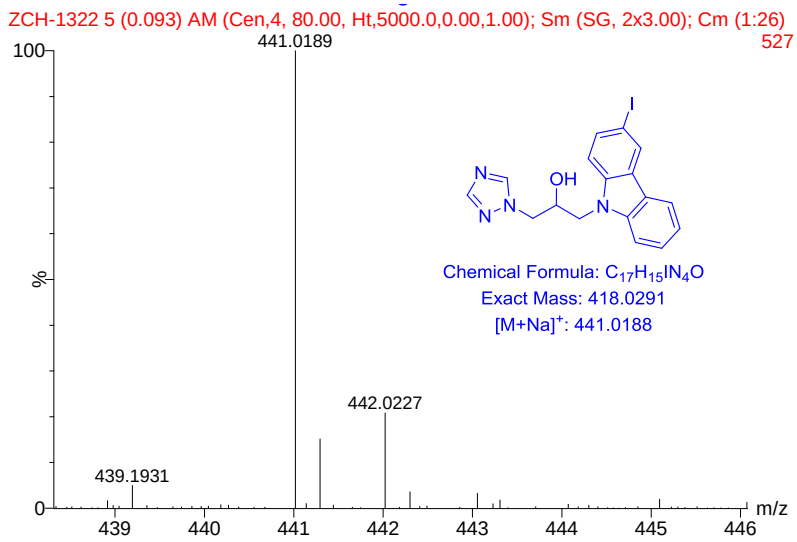

Figure S23. HRMS spectrum of compound **3d**

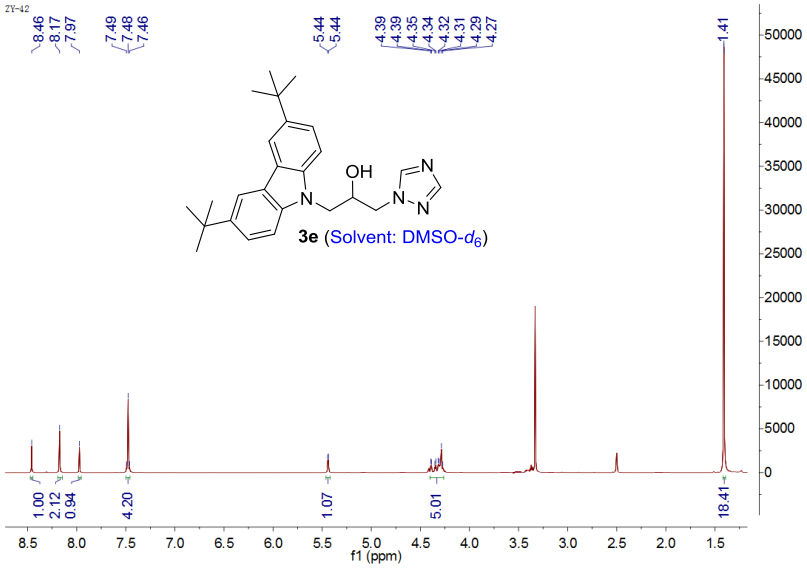

Figure S24. ^{1}H NMR spectrum of compound **3e**

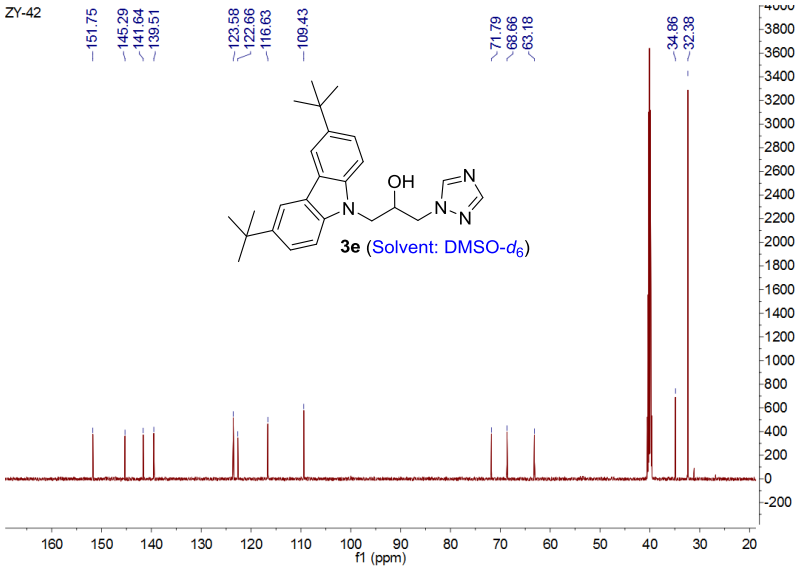

Figure S25. ^{13}C NMR spectrum of compound **3e**

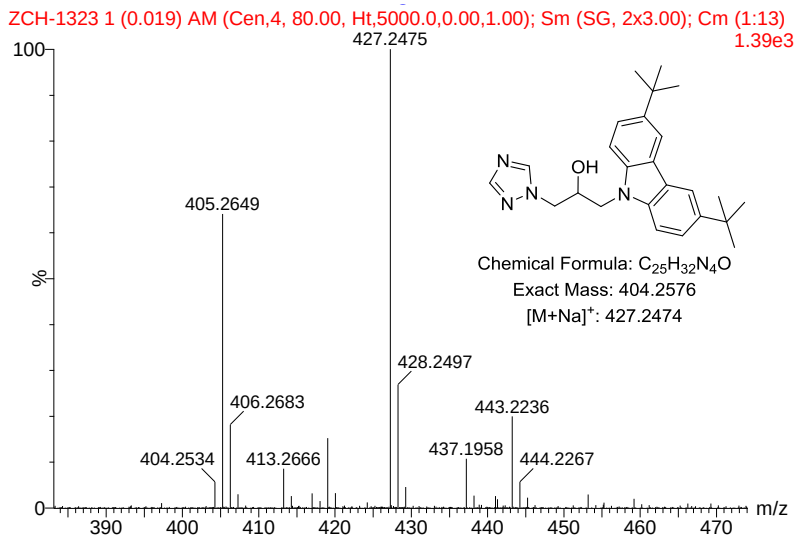

Figure S26. HRMS spectrum of compound **3e**

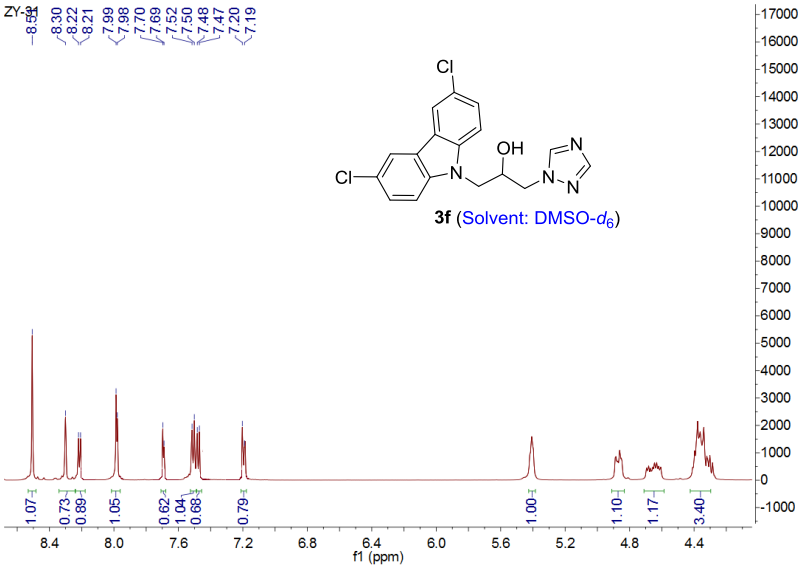

Figure S27. ^{1}H NMR spectrum of compound **3f**

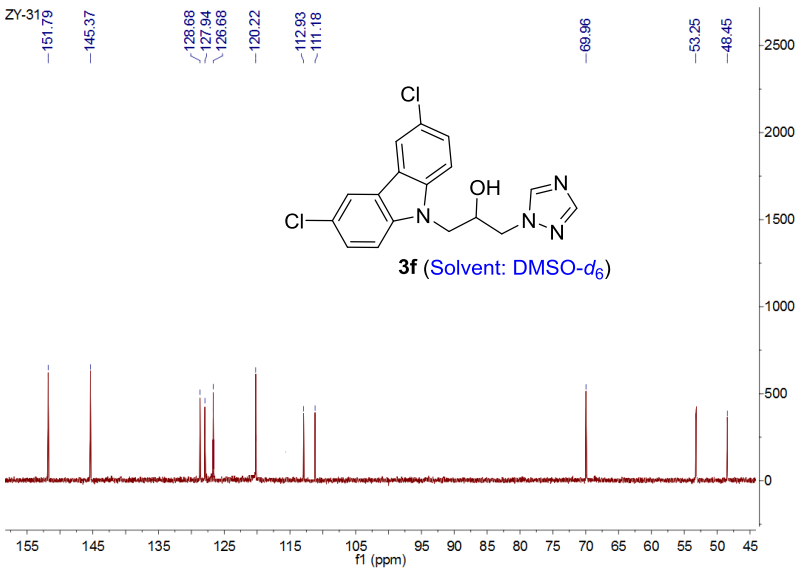

Figure S28. ^{13}C NMR spectrum of compound **3f**

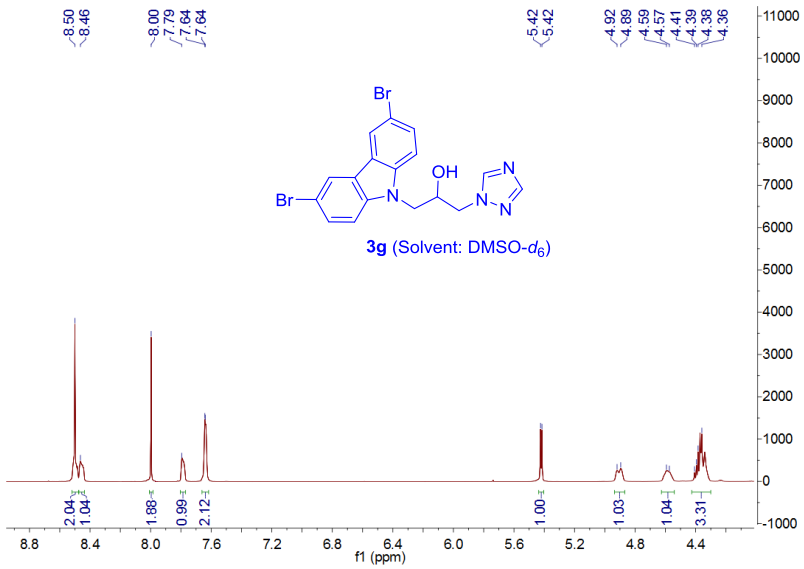

Figure S29. ^{1}H NMR spectrum of compound **3g**

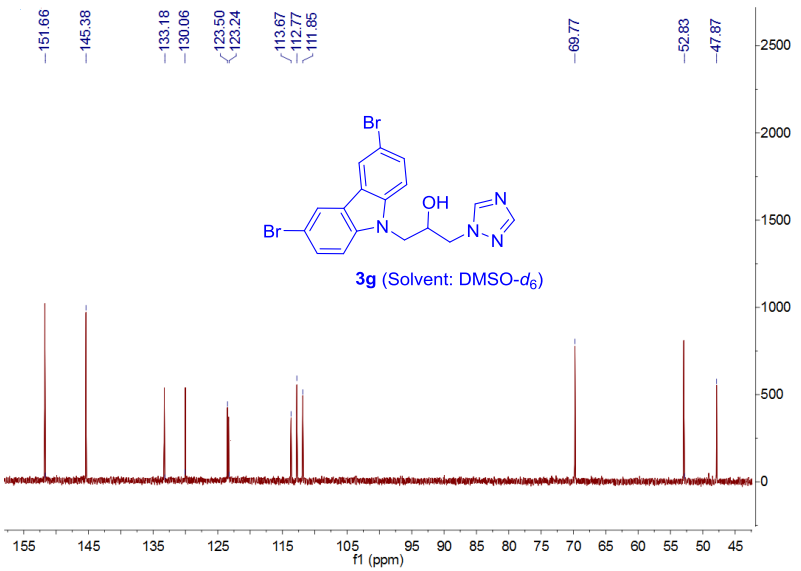

Figure S30. ^{13}C NMR spectrum of compound **3g**

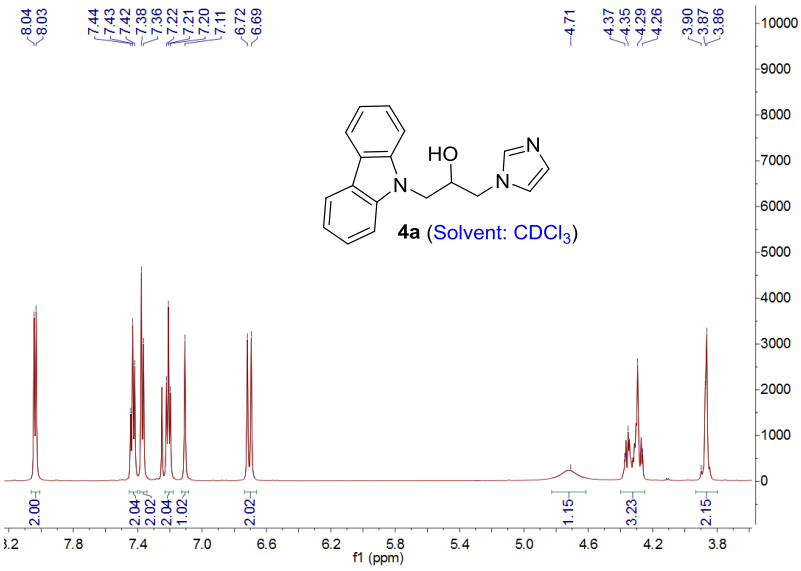

Figure S31. ^{1}H NMR spectrum of compound **4a**

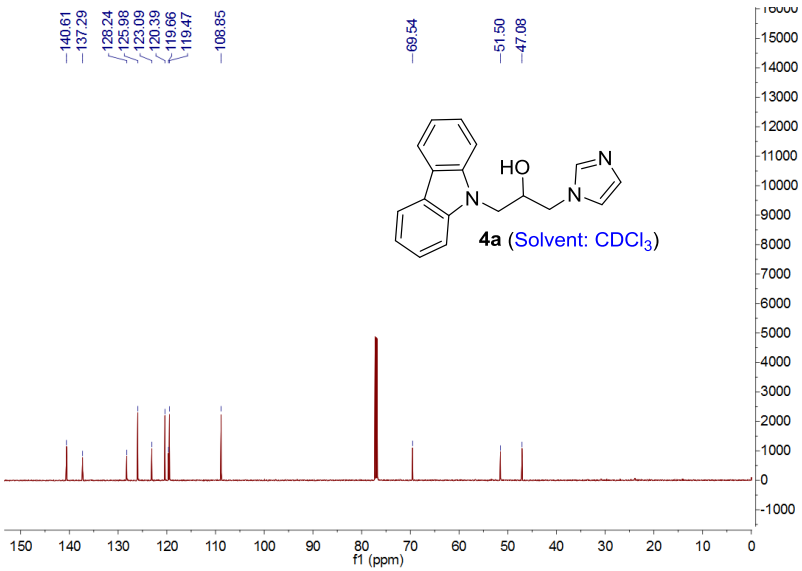

Figure S32. ^{13}C NMR spectrum of compound **4a**

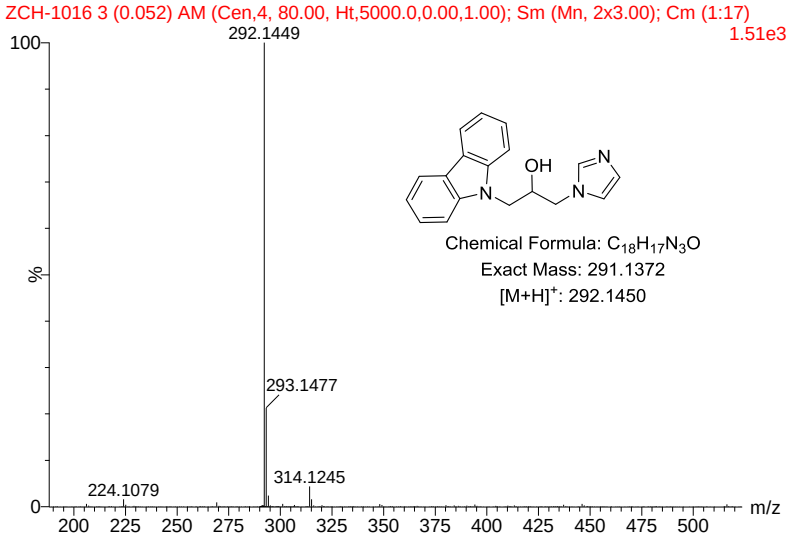

Figure S33. HRMS spectrum of compound **4a**

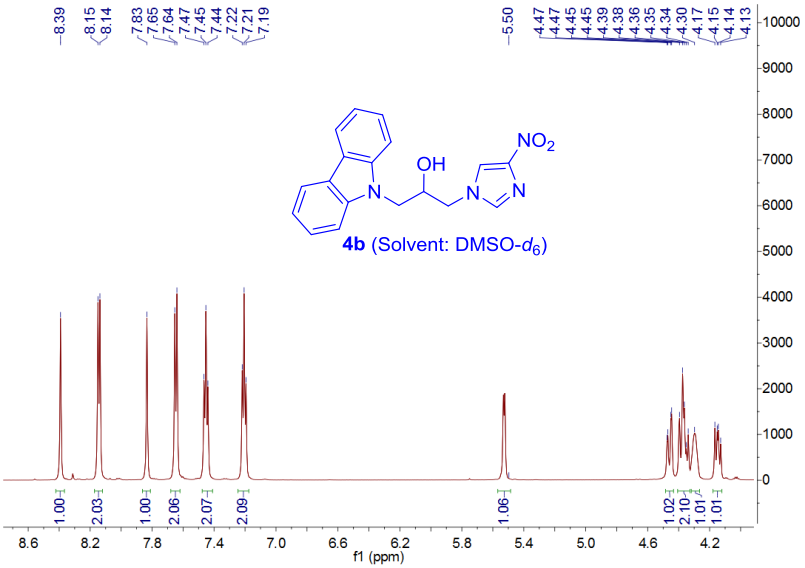

Figure S34. ^{1}H NMR spectrum of compound **4b**

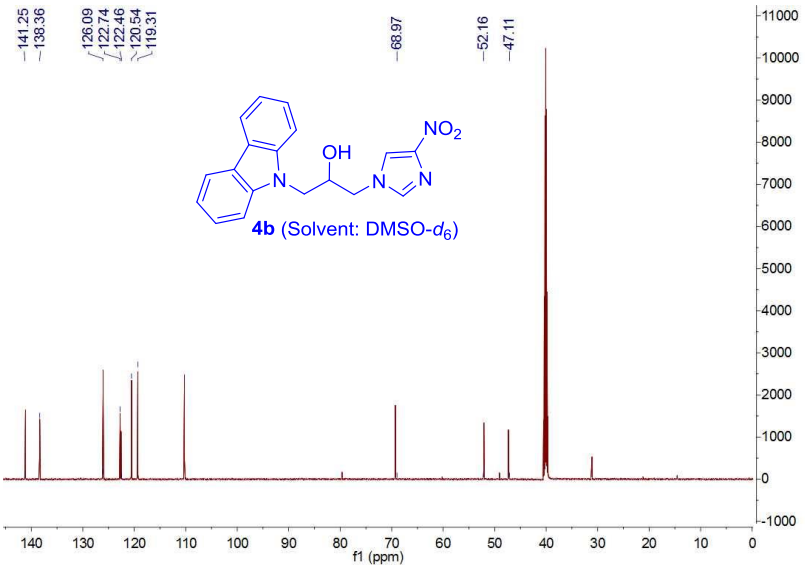

Figure S35. ^{13}C NMR spectrum of compound **4b**

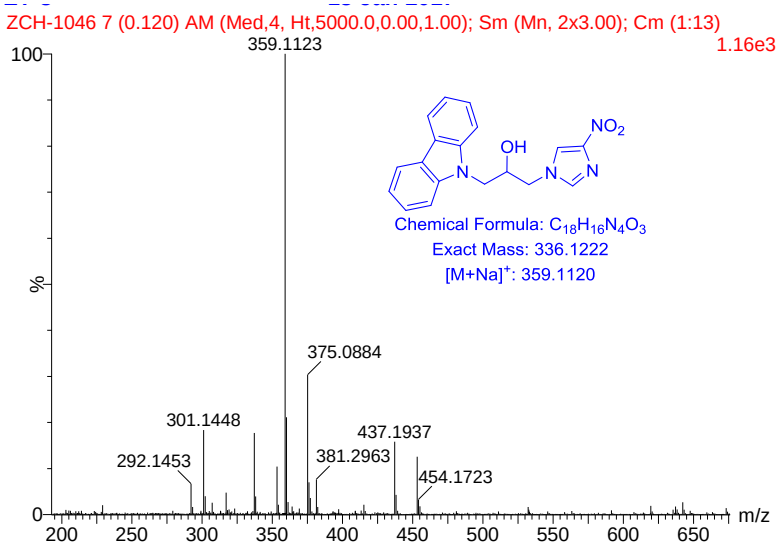

Figure S36. HRMS spectrum of compound **4b**

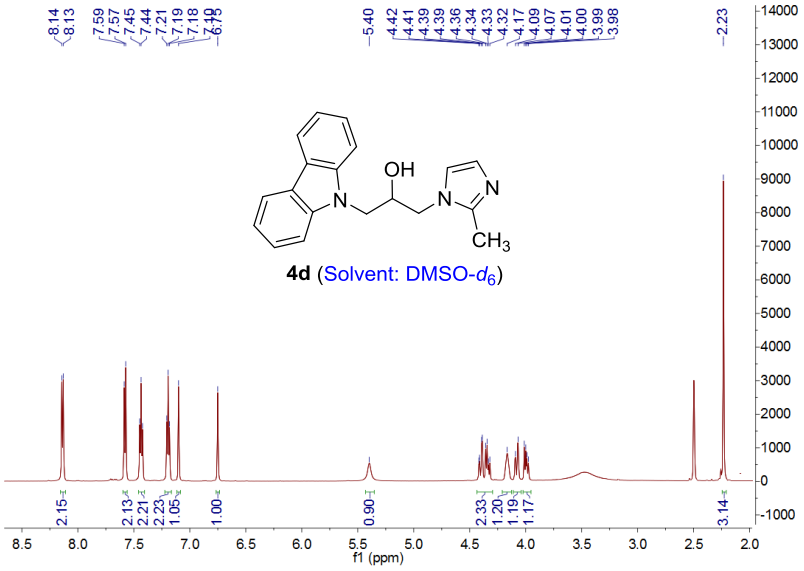

Figure S37. ^{1}H NMR spectrum of compound **4d**

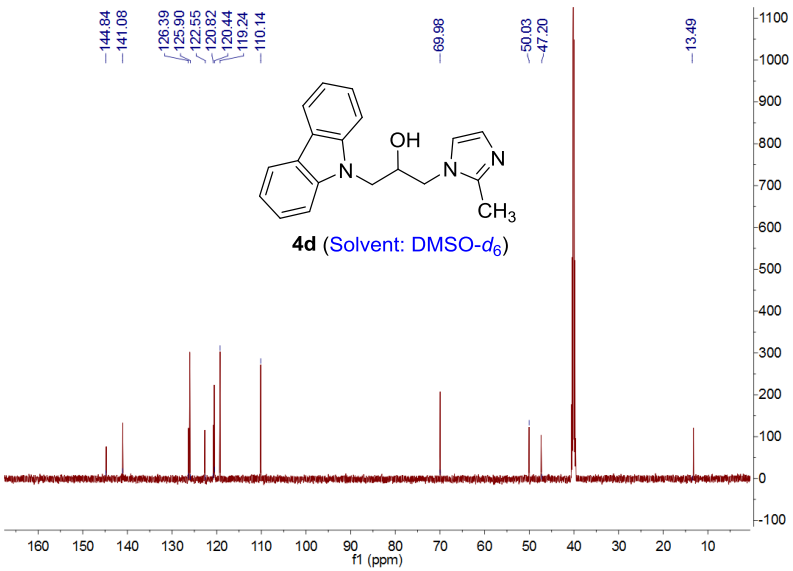

Figure S38. ^{13}C NMR spectrum of compound **4d**

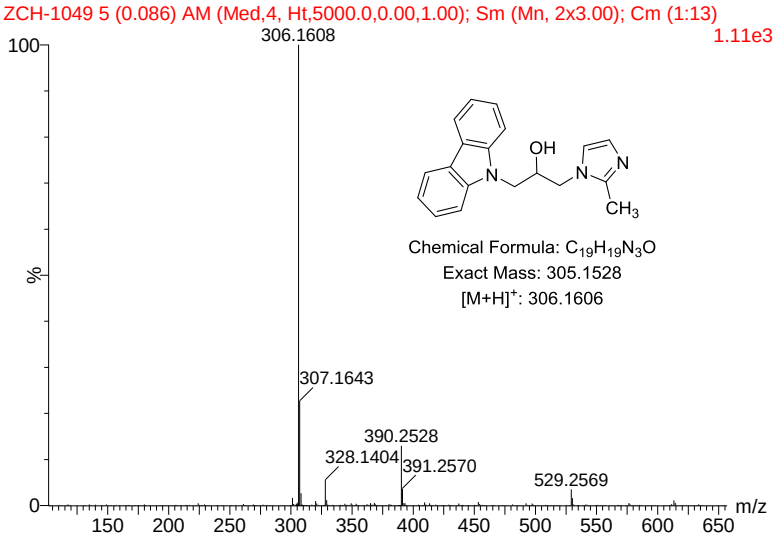

Figure S39. HRMS spectrum of compound **4d**

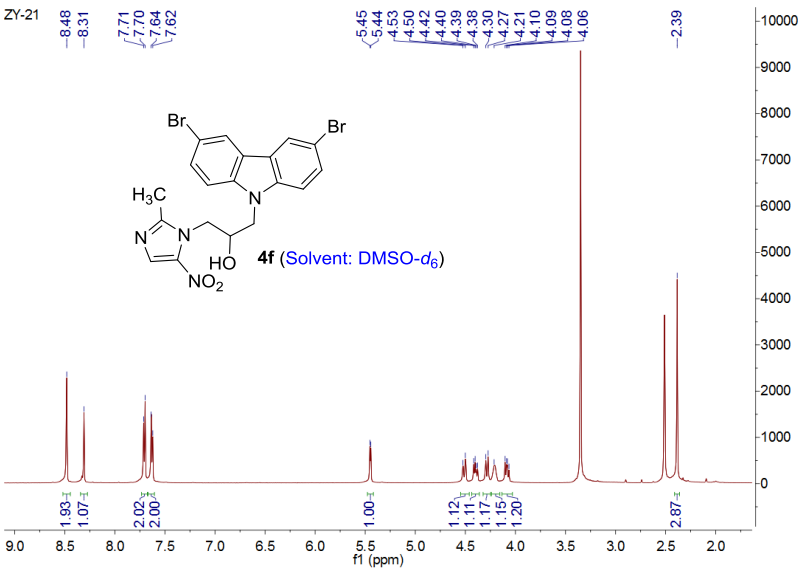

Figure S40. ^{1}H NMR spectrum of compound **4f**

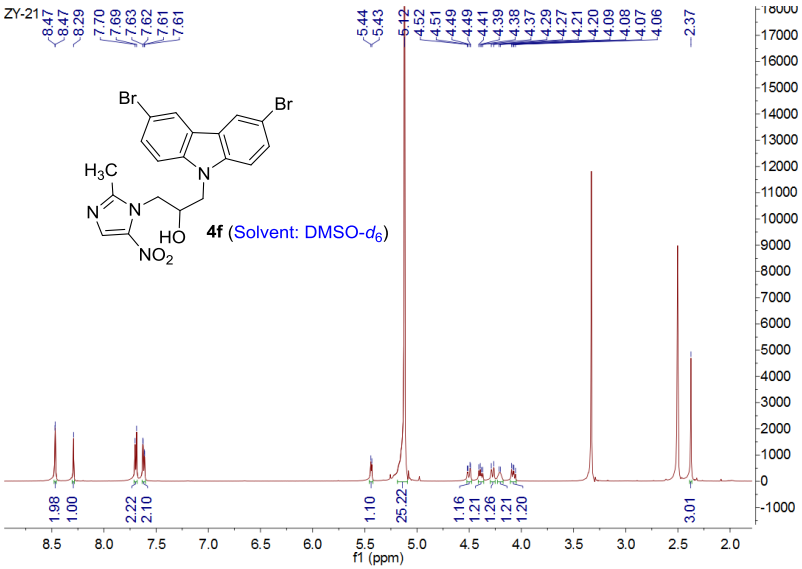

Figure S41. QNMR spectrum of compound **4f**

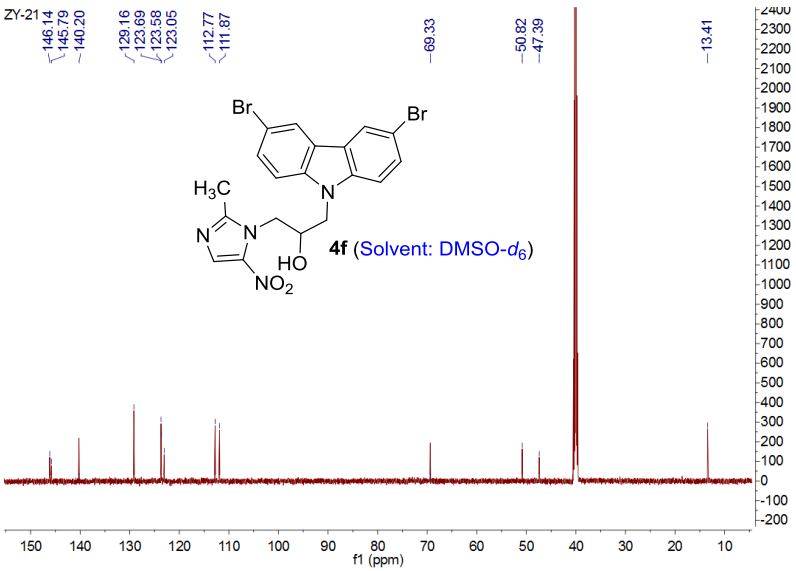

Figure S42. ^{13}C NMR spectrum of compound **4f**

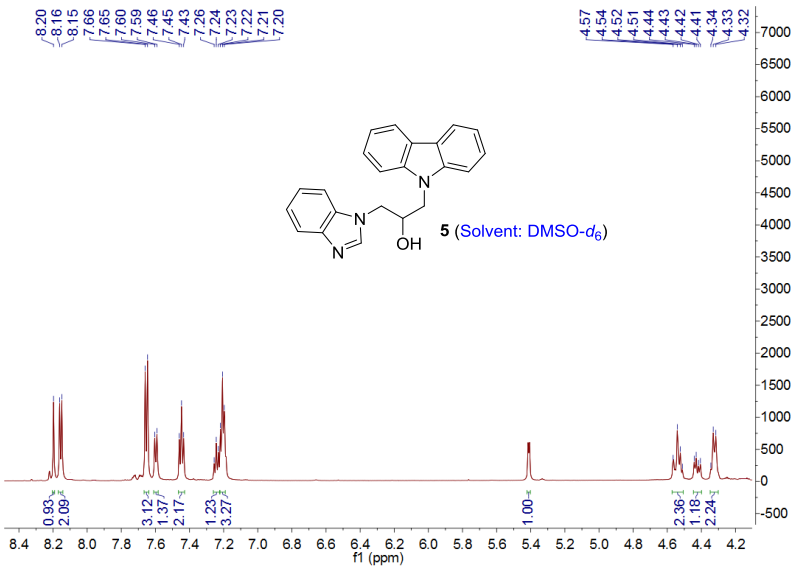

Figure S43. ^{1}H NMR spectrum of compound **5**

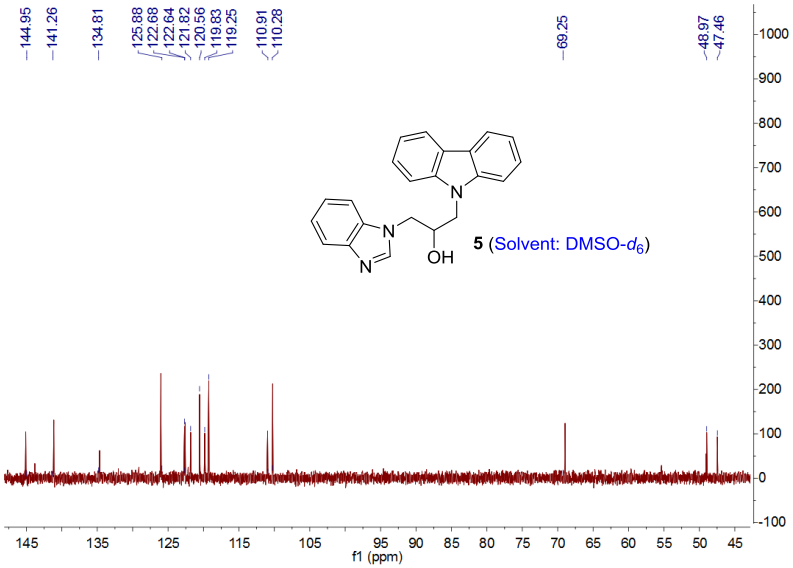

Figure S44. ^{13}C NMR spectrum of compound **5**

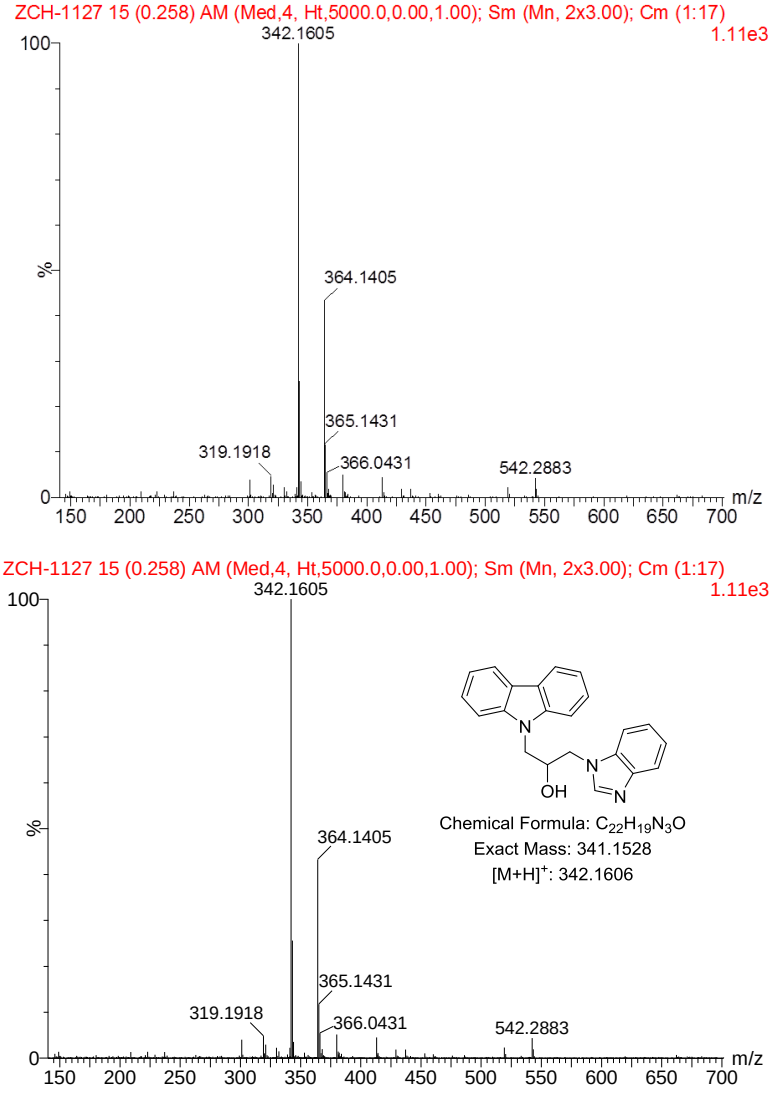

Figure S45. HRMS spectrum of compound **5**

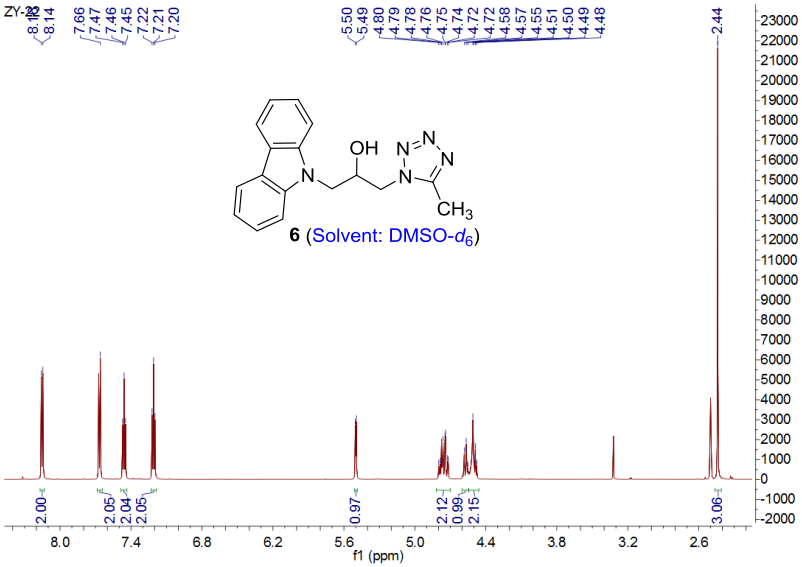

Figure S46. ^{1}H NMR spectrum of compound **6**

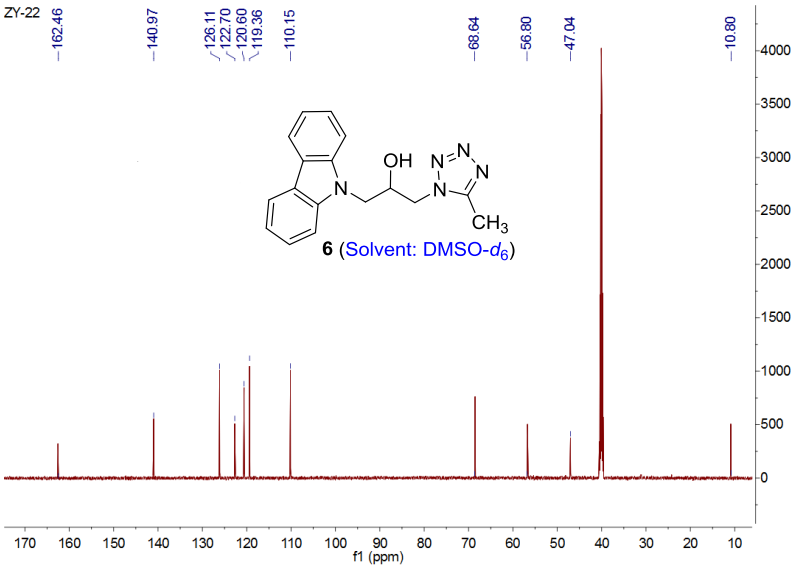

Figure S47. ^{13}C NMR spectrum of compound **6**

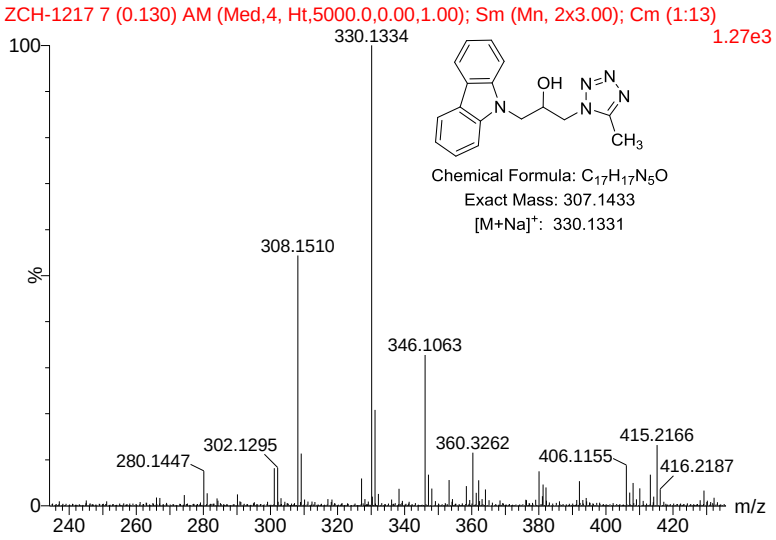

Figure S48. HRMS spectrum of compound **6**

REFERENCES

(1) Li, X. L.; Hu, Y. J.; Wang H.; Yu, B. Q.; Yue, H. L. Molecular Spectroscopy Evidence of Berberine Binding to DNA: Comparative Binding and Thermodynamic Profile of Intercalation. *Biomacromolecules* **2012**, *13*, 873–880.

(2) Wen, S. Q.; Ponmani, J.; Avula, S. R.; Zhang, L.; Zhou, C. H. Discovery of Novel Berberine Imidazoles as Safe Antimicrobial Agents by Down Regulating ROS Generation. *Bioorg. Med. Chem. Lett.* **2016**, *26*, 2768–2773.

(3) Akbay, N.; Seferoğlu, Z.; Gök, E. Fluorescence Interaction and Determination of Calf Thymus DNA with Two Ethidium Derivatives. *J. Fluoresc.* **2009**, *19*, 1045–1051.

(4) Zhang, L.; Kumar, K. V.; Rasheed, S.; Zhang, S. L.; Geng, R. X.; Zhou, C. H. Design, Synthesis, and Antibacterial Evaluation of Novel Azolylthioether Quinolones as MRSA DNA Intercalators. *MedChemComm* **2015**, *6*, 1303–1310.

(5) Peng, X. M.; Peng, L. P.; Li, S.; Avula, S. R.; Kumar, K. V.; Zhang, S. L.; Tam, K. Y.; Zhou, C. H. Quinazolinone Azolyl Ethanols: Potential Lead Antimicrobial Agents with Dual Action Modes Targeting Methicillin-resistant *Staphylococcus aureus* DNA. *Future Med. Chem.* **2016**, *8*, 1927–1940.